



Det här verket är upphovrättskyddat enligt *Lagen (1960:729) om upphovsrätt till litterära och konstnärliga verk*. Det har digitaliserats med stöd av Kap. 1, 16 § första stycket p 1, för forskningsändamål, och får inte spridas vidare till allmänheten utan upphovsrättsinnehavarens medgivande.

Alla tryckta texter är OCR-tolkade till maskinläsbar text. Det betyder att du kan söka och kopiera texten från dokumentet. Vissa äldre dokument med dåligt tryck kan vara svåra att OCR-tolka korrekt vilket medför att den OCR-tolkade texten kan innehålla fel och därför bör man visuellt jämföra med verkets bilder för att avgöra vad som är riktigt.

This work is protected by Swedish Copyright Law (*Lagen (1960:729) om upphovsrätt till litterära och konstnärliga verk*). It has been digitized with support of Kap. 1, 16 § första stycket p 1, for scientific purpose, and may no be disseminated to the public without consent of the copyright holder.

All printed texts have been OCR-processed and converted to machine readable text. This means that you can search and copy text from the document. Some early printed books are hard to OCR-process correctly and the text may contain errors, so one should always visually compare it with the images to determine what is correct.

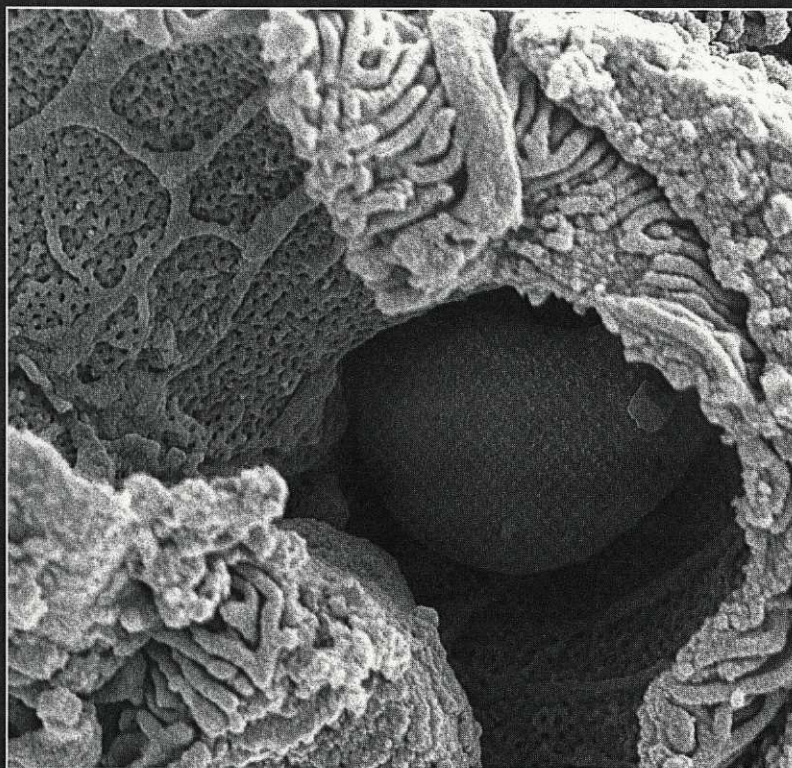


GÖTEBORGS UNIVERSITETSBIBLIOTEK



100148 7023

Aspects of the Glomerular Barrier in Healthy and Diabetic Kidneys



Marie Jeansson



SAHLGRENKA ACADEMY
GÖTEBORG UNIVERSITY
SWEDEN 2005

RENALCENTER
RESEARCH CARE EDUCATION



Biomedicinska biblioteket



Aspects of the Glomerular Barrier in Healthy and Diabetic Kidneys

AKADEMISK AVHANDLING

som för avläggande av medicine doktorexamen vid Göteborgs Universitet
kommer att offentligen försvaras i Akademicums föreläsningssal, Arvid Carlsson,
Medicinaregatan 1, fredagen den 20 maj 2005, klockan 9.00

av

Marie Jeansson
Fil. Mag.

Avhandlingen baseras på följande arbeten:

- I. Glomerular size and charge selectivity in the mouse after exposure to glucosaminoglycan degrading enzymes.
Marie Jeansson & Börje Haraldsson
J Am Soc Nephrol. 14: 1756-1765, 2003
- II. Evidence for the importance of the endothelial cell glycocalyx in the glomerular barrier.
Marie Jeansson & Börje Haraldsson
Submitted
- III. Functional and molecular alterations of the glomerular barrier in long term diabetes in mice.
Marie Jeansson, Anna Björnson Granqvist, Jenny Nyström
& Börje Haraldsson
Submitted

Fakultetsopponent:

Professor Andrea Remuzzi, Mario Negri Institute, Bergamo, Italy

ABSTRACT

Jeansson, M. Aspects of the glomerular barrier in healthy and diabetic kidneys. The Renal Center, Departments of Physiology and Nephrology, Göteborg University, SE-405 30 Göteborg, Sweden

Each day 180 liters of plasma is filtered in the kidneys. Under normal conditions, the glomerular barrier restricts the passage of macromolecules such as albumin while it is highly permeable to water and small solutes. Proteinuria is a hallmark of renal disease and reflects impairment of the glomerular barrier. The glomerular barrier has size and charge selective properties and consists of the fenestrated endothelium covered with a glycocalyx, the glomerular basement membrane, and the podocytes.

In this thesis, the somewhat controversial issue of involvement of the endothelial cell glycocalyx in glomerular charge selectivity is investigated. The glomerular barrier has been studied with respect to function, morphology and gene expression in healthy, enzyme treated, and diabetic kidneys. Experiments were performed using the isolated perfused kidneys at 8°C in order to investigate the glomerular barrier without the tubular modifications of primary urine that occurs *in vivo*.

Kidneys in which the endothelial cell glycocalyx was altered with glucose/galactoseaminoglycan (GAG) degrading enzymes showed an up to 5-fold increase in fractional clearance for albumin. This is due to an alteration in glomerular charge selectivity since the fractional clearance for Ficoll 35.5 Å, the neutral counterpart of albumin, was unaltered. The enzyme action on the glycocalyx was confirmed morphologically in electron microscopy where Intralipid® droplets were used as indirect markers of the glycocalyx.

To clarify if long term diabetes alters glomerular size or charge selectivity or both, we studied non obese diabetic mice for 10 and 40 weeks. Diabetes for 40 weeks resulted in altered glomerular charge selectivity as shown by a 3-fold increase in the fractional clearance for albumin, without any change of the neutral counterpart Ficoll 35.5 Å. Real-time PCR with the low density arrays revealed a down-regulation of cortex mRNA expression for versican, decorin, biglycan, matrix metalloprotease-9, and podocin after 40 weeks of diabetes.

In summary, this thesis describes the importance of the glomerular endothelial cell glycocalyx in charge selectivity. In addition, albuminuria in long term diabetes originates from an alteration in charge selectivity which is coupled to down-regulation of the glycocalyx component, versican.

Keywords: glomerular size and charge selectivity • isolated perfused kidney • electron microscopy • glycocalyx • diabetic nephropathy • NOD mice

ISBN: 91-628-6485-8

Aspects of the Glomerular Barrier in Healthy and Diabetic Kidneys



Marie Jeansson



SAHLGRENSKA ACADEMY
GÖTEBORG UNIVERSITY
SWEDEN 2005

RENALCENTER
RESEARCH CARE EDUCATION



Cover description:

Scanning electron micrograph of a glomerular capillary. The capillary with its fenestrated endothelium contains a red blood cell.

ISBN 91-628-6485-8

© 2005 Marie Jeansson

Printed in Sweden by Intellecta DocuSys AB, Göteborg

Till mamma

ABSTRACT

Jeansson, M. Aspects of the glomerular barrier in healthy and diabetic kidneys. The Renal Center, Departments of Physiology and Nephrology, Göteborg University, SE-405 30 Göteborg, Sweden

Each day 180 liters of plasma is filtered in the kidneys. Under normal conditions, the glomerular barrier restricts the passage of macromolecules such as albumin while it is highly permeable to water and small solutes. Proteinuria is a hallmark of renal disease and reflects impairment of the glomerular barrier. The glomerular barrier has size and charge selective properties and consists of the fenestrated endothelium covered with a glycocalyx, the glomerular basement membrane, and the podocytes.

In this thesis, the somewhat controversial issue of involvement of the endothelial cell glycocalyx in glomerular charge selectivity is investigated. The glomerular barrier has been studied with respect to function, morphology and gene expression in healthy, enzyme treated, and diabetic kidneys. Experiments were performed using the isolated perfused kidneys at 8°C in order to investigate the glomerular barrier without the tubular modifications of primary urine that occurs in vivo.

Kidneys in which the endothelial cell glycocalyx was altered with glucose/galactoseaminoglycan (GAG) degrading enzymes showed an up to 5-fold increase in fractional clearance for albumin. This is due to an alteration in glomerular charge selectivity since the fractional clearance for Ficoll 35.5 Å, the neutral counterpart of albumin, was unaltered. The enzyme action on the glycocalyx was confirmed morphologically in electron microscopy where Intralipid® droplets were used as indirect markers of the glycocalyx.

To clarify if long term diabetes alters glomerular size or charge selectivity or both, we studied non obese diabetic mice for 10 and 40 weeks. Diabetes for 40 weeks resulted in altered glomerular charge selectivity as shown by a 3-fold increase in the fractional clearance for albumin, without any change of the neutral counterpart Ficoll 35.5 Å. Real-time PCR with the low density arrays revealed a down-regulation of cortex mRNA expression for versican, decorin, biglycan, matrix metalloprotease-9, and podocin after 40 weeks of diabetes.

In summary, this thesis describes the importance of the glomerular endothelial cell glycocalyx in charge selectivity. In addition, albuminuria in long term diabetes originates from an alteration in charge selectivity which is coupled to down-regulation of the glycocalyx component, versican.

Keywords: glomerular size and charge selectivity • isolated perfused kidney • electron microscopy • glycocalyx • diabetic nephropathy • NOD mice

ISBN: 91-628-6485-8

LIST OF PUBLICATIONS

This thesis is based upon the following papers, which are referred to in the text by their Roman numerals:

- I. **Glomerular size and charge selectivity in the mouse after exposure to glucosaminoglycan degrading enzymes.**
Marie Jeansson & Börje Haraldsson
J Am Soc Nephrol. 14: 1756-1765, 2003

- II. **Evidence for the importance of the endothelial cell glycocalyx in the glomerular barrier.**
Marie Jeansson & Börje Haraldsson
Submitted

- III. **Functional and molecular alterations of the glomerular barrier in long term diabetes in mice.**
Marie Jeansson, Anna Björnson Granqvist, Jenny Nyström & Börje Haraldsson
Submitted

ABBREVIATIONS

Å	Ångström (0.1 nm)
ACEi	angiotensin converting enzyme inhibitor
ARB	angiotensin receptor blocker
Chond	chondroitinase
cIPK	cooled isolated perfused kidney
C _P	plasma concentration
C _U	urine concentration
EM	electron microscopy
ESRD	end-stage renal disease
FITC	fluorescein isothiocyanate
GAG	glucose/galactoseaminoglycan
GBM	glomerular basement membrane
GFR	glomerular filtration rate
h	hour
HD	high dose
Hep	heparinase
HPLC	high performance liquid chromatography
HRP	horse radish peroxidase
HSA	human serum albumin
Hya	hyaluronidase
kDa	kilo Dalton
LD	low dose
mEq/L	milli equivalents per liter
MMP	matrix metalloprotease
NOD	non obese diabetic
PCR	polymerase chain reaction
SLRP	small leucine-rich proteoglycans
RT	room temperature

SYMBOLS

θ	fractional clearance
$A_0/\Delta x$	unrestricted exchange area over diffusion distance
f_L	large pore fraction of the glomerular filtrate

Charged fiber model

q_f	surface charge density of the fiber
q_s	surface charge density of the solute
r_f	fiber radius
r_L	large pore radius
r_s	solute radius
ϕ	volume fraction of fibers

Gel-membrane model

ω	charge density
r_s	small pore radius
r_L	large pore radius

CONTENTS

ABSTRACT	i
LIST OF PUBLICATIONS	ii
ABBREVIATIONS	iii
INTRODUCTION	1
The glomerular barrier	1
Endothelial cell glycocalyx	2
Diabetes	4
Diabetic nephropathy	4
Animal models of diabetic nephropathy	6
AIMS	7
MATERIALS AND METHODS	8
Animals	8
Anesthesia	8
Enzymes (papers I & II)	8
Tail-cuff plethysmography (paper III)	9
Glomerular barrier studies	9
<i>Tracers (papers I-III)</i>	9
<i>In vivo (paper I)</i>	9
<i>The cooled isolated perfused kidney model, cIPK (papers I-III)</i>	10
<i>Perfusate (papers I-III)</i>	10
<i>Data analysis (papers I-III)</i>	11
<i>Analysis of Ficoll (papers I-III)</i>	11
Models of the Glomerular Barrier	11
<i>The heterogeneous charged fiber model (paper I)</i>	11
<i>The gel-membrane model (paper I-III)</i>	12
<i>Lognormal distribution + shunt model (paper I)</i>	12
Glomerular morphology	13
<i>General morphology (paper I)</i>	13
<i>Glycocalyx estimation (paper II)</i>	13
<i>Glomerular basement membrane thickness (paper III)</i>	13
<i>Glomerular size and sclerosis (paper III)</i>	14
Protein and mRNA expression (paper III)	14
<i>Quantitative Real-time PCR</i>	14
<i>Immunohistochemistry</i>	16
<i>Western blot</i>	16
Calculations	17
<i>Glomerular filtration rate (GFR)</i>	17
<i>Fractional clearance, θ</i>	17
<i>Quantification of mRNA</i>	17
Statistics	18

REVIEW OF RESULTS	19
The cIPK model versus in vivo	19
Endothelial cell glycocalyx in the glomerular barrier (paper I, II).....	20
<i>Functional aspects.....</i>	<i>20</i>
<i>Morphological aspects.....</i>	<i>21</i>
The Glomerular Barrier in Diabetes (paper III)	22
<i>Diabetic Nephropathy in the NOD mouse</i>	<i>22</i>
<i>Functional aspects.....</i>	<i>23</i>
<i>Molecular aspects</i>	<i>24</i>
DISCUSSION.....	26
In vivo versus the cIPK	26
Mathematical models.....	27
Endothelial cell glycocalyx and charge selectivity.....	28
The glomerular barrier in diabetes	29
Gene regulation in diabetic nephropathy	30
<i>Versican.....</i>	<i>30</i>
<i>Decorin.....</i>	<i>31</i>
<i>MMP-9</i>	<i>31</i>
<i>Podocin.....</i>	<i>31</i>
Therapies in diabetic nephropathy	32
CONCLUDING REMARKS	33
FUTURE PERSPECTIVES	33
SVENSK SAMMANFATTNING	34
ACKNOWLEDGEMENTS	35
REFERENCES.....	36

INTRODUCTION

Every human kidney has around 1 million nephrons, the functional unit of the kidney. Every day 180 liters of plasma is filtered over the glomerular capillary wall creating the same amount of primary urine. The primary urine is modified during the passage of the tubules giving a final urine volume of 1-2 liters. Under normal conditions, the glomerular barrier restricts the passage of macromolecules such as albumin while it is highly permeable to water and small solutes. Proteinuria is a hallmark of renal disease and reflects impairment of the glomerular barrier. This thesis is focused on the production of primary urine and the properties of the glomerular filtration barrier.

The glomerular barrier

The glomerular barrier consists of 3 layers (Figure 1): 1) the fenestrated endothelium covered with a glycocalyx, 2) the glomerular basement membrane (GBM), and 3) the podocyte foot processes. Classical studies have demonstrated both in vivo and in vitro that the glomerular barrier restricts the passage of anionic macromolecules relative to uncharged ones of similar size and configuration (17, 24, 133, 134). There are, however, investigators suggesting that the effects of solute charge are negligible (125, 143).

Our group has carried out extensive studies using Ficolls and various neutral and charged proteins. The results show that the glomerular barrier is indeed highly size and charge selective (76, 96, 119, 121, 163). The structures responsible for glomerular size and charge selectivity are also under debate. Several novel proteins in the podocyte slit diaphragm such as nephrin, podocin, and CD2AP have been identified (137, 142, 156). They have been shown to be important for barrier function

since mutations in the genetic code for each of the proteins are connected to nephrotic syndromes (15, 83, 157, 168). The podocyte slit diaphragm is considered by many investigators to be the main size selective barrier (168). The GBM consists mainly of collagen IV, laminin, nidogen, and proteoglycans and has for a long time been considered to be the main barrier in glomerular filtration. Studies using electron microscopy and different cationic probes such as ferritin (80, 81, 133) and lysozyme (23) have demonstrated the presence of anionic charges in the GBM. When anionic probes tended to be excluded from the GBM, it was suggested to be

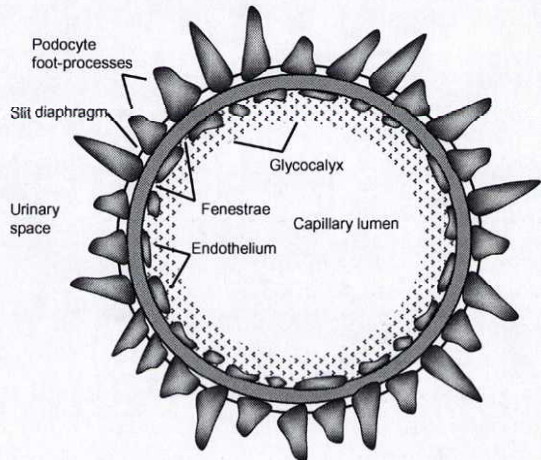


Figure 1. A schematic figure of the glomerular barrier.

the location for charge selectivity. However, anionic sites have also been demonstrated on the endothelial (133, 182) and the epithelial cells (56). Also, functional studies on filtration across isolated GBM have shown much less charge selectivity than in *in vivo* or in isolated glomeruli (12, 16, 34). This suggests that charge selectivity resides mainly at endothelial or epithelial cells or that charged structures are lost in the process of isolating the GBM. In addition, our group has suggested a role for the glomerular endothelial cell glycocalyx in charge selectivity (7, 30, 60, 67, 76, 120, 164), an idea supported by others (5, 40). Furthermore, our group has found that charge selectivity can be reversibly altered by changing perfusate ionic strength (30, 164), but not when changing osmolality (97). In addition, we have shown that glomerular permeability is affected by plasma composition (61, 78), supporting the idea of an intimate relation between charge selectivity and plasma proteins.

Endothelial cell glycocalyx

Endothelial cells are covered with a surface layer of membrane-associated and secreted proteoglycans, glucosaminoglycans, glycoproteins, glycolipids, and associated plasma proteins. This is known as the glycocalyx or the endothelial surface layer (130). The composition and the physical properties of the glycocalyx, including the effective thickness, seem to be influenced by the adsorption of plasma proteins (130, 131). Both albumin and orosomucoid (α_1 -acid glycoprotein) are reported to bind microvascular endothelial cells in culture (126, 145-147). We have shown that orosomucoid is important for glomerular permeability (61, 78). The endothelial glycocalyx have a surprisingly large *in vivo* thickness as well as certain permselective properties as Duling and coworkers showed by combining intravital brightfield and fluorescence microscopy (65, 179, 180). These authors estimated that the glycocalyx in cremaster muscle capillaries was 400-500 nm thick by subtracting the width of the fluorescent tracer column from the anatomical diameter (180). Hence, the glycocalyx appears to be much thicker than estimated from electron microscopy, 50-100 nm (130), which likely underestimates the thickness due to the dehydration following tissue fixation. Problems in

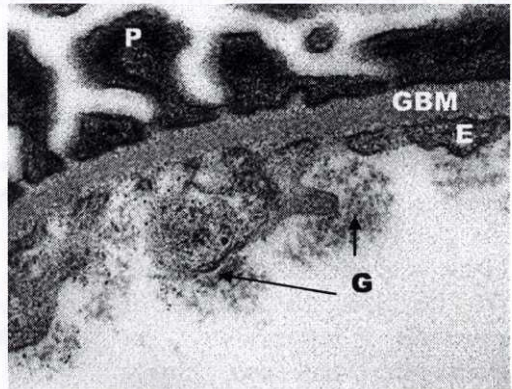


Figure 2. An electron micrograph of the glomerular barrier of a rat. Seen are podocytes (P) with the slit diaphragm in between, the glomerular basement membrane (GBM), and the endothelium (E) with the glycocalyx (G). The glycocalyx is visualized with tannic acid and uranyl acetat.

Courtesy of Dr. Clara Hjalmarsson

visualizing the glycocalyx are probably the reason why the glycocalyx has been overlooked when considering microvascular permeability and exchange. However, recent studies where vascular beds were perfused with a fluorocarbon-based oxygen carrying fixative, followed by contrast enhancing preparation steps, showed a delicate ~60-300 nm thick glycocalyx on the glomerular endothelium and its fenestrae, see Figure 2 (67, 139, 140). As mentioned, the glycocalyx consists of proteoglycans, glucosaminoglycans, glycoproteins, glycolipids, and associated plasma proteins. Proteoglycans consists of a protein core to which one or several chains of repeating disaccharide chains are attached. The repeating disaccharides can be either glucose- or galactoseaminoglycans (GAG). The GAG chains are negatively charged due to carboxyl groups and/or sulfate groups. The proteoglycan versican have the GAG chains chondroitin sulfate attached to its protein core.

Versican is an extracellular proteoglycan that can bind to hyaluronic acid and be stimulated by growth factors such as platelet derived growth factor (PDGF) and transforming growth factor- β_1 (TGF- β_1) (175). Perlecan and agrin are the main proteoglycans in glomerular basement membranes (57). They both carry the GAG heparan sulfate, though perlecan sometimes have

chondroitin sulfate (74). Other extracellular proteoglycans are the small leucine-rich proteoglycans (SLRP) such as decorin, biglycan, and fibromodulin. Decorin and biglycan have one or two GAG chains of chondroitin/dermatan sulfate attached, while fibromodulin have keratan sulfate (73). Several SLRPs have been shown to bind TGF- β (66, 183). The glypicans carry the GAG chains heparan sulfate and are linked to the plasma membrane through a covalent glycosyl-phosphatidylinositol (GPI) anchor (35). Syndecans are transmembrane proteoglycans that generally have the GAG chains heparan sulfate attached. However, some isoforms may contain chondroitin sulfate. Hyaluronic acid is an unsulfated glucosaminoglycan without a protein core. It can form large aggregates and be attached to the cell surface via receptors such as RHAMM (receptor for hyaluronic acid mediated motility), CD44, and ICAM-1 (95, 105, 170).

Studies of the negatively charged components in the glomerular endothelial cell glycocalyx are incomplete, but there are indirect evidence for involvement of hyaluronic acid (5, 76), heparan sulfate (5), chondroitin sulfate (76), and sialoproteins (5). In addition, our group has recently shown that human glomerular

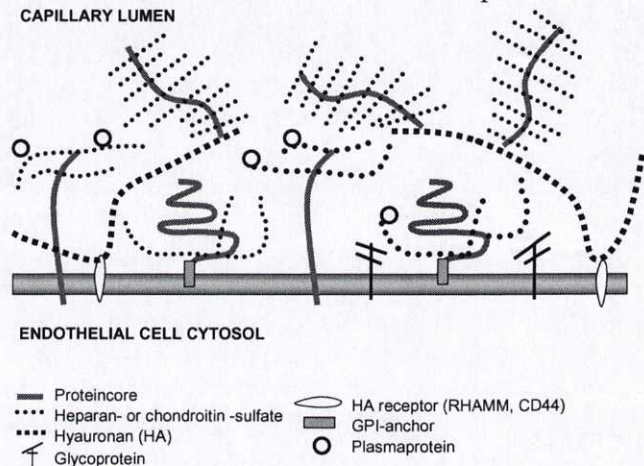


Figure 3. A schematic figure of the endothelial cell glycocalyx.

endothelial cells produce several different proteoglycans such as syndecan, versican, glypican, perlecan, decorin, and biglycan (7). Also, we have shown that hyaluronic acid and/or chondroitin sulfate in the glomerular endothelial cell glycocalyx are important to maintain charge selective properties of the glomerular barrier (76). A schematic diagram of the glomerular endothelial cell glycocalyx is shown in Figure 3.

Diabetes

Diabetes mellitus is a group of diseases characterized by high levels of blood glucose, resulting from defects in insulin production, insulin action, or both. Type 1 diabetes (insulin-dependent diabetes mellitus, juvenile-onset diabetes) develops when the insulin producing β -cells are destroyed by the immune system. Diabetes type 1 may account for 5-10 % of all diagnosed cases of diabetes (114). Possible risk factors for type 1 diabetes are autoimmune, genetic, and environmental factors. Type 2 diabetes (non-insulin-dependent diabetes mellitus, adult-onset diabetes) may account for about 90-95 % of all diagnosed cases of diabetes (114). It usually begins as insulin resistance, a disorder in which the cells do not utilize insulin properly. As the need for insulin increases, the pancreas gradually loses its ability to produce insulin. Diabetes type 2 is associated with older age, obesity, family history of diabetes, history of gestational diabetes, impaired glucose metabolism, and physical inactivity. Type 2 diabetes is increasingly being diagnosed in children and adolescents (49, 98). Gestational diabetes is a form of glucose intolerance that is diagnosed in some women during pregnancy. Women who have had gestational diabetes have a 20-50 % risk of developing diabetes in the following 5-10 years (114). Diabetes can affect many parts of the body and can lead to serious complications such as retinopathy, nephropathy and neuropathy. Diabetic patients also have an increased risk of cardiovascular disease and approximately 65 % of deaths among diabetic patients are due to cardiovascular disease and stroke (3, 59, 72).

Diabetic nephropathy

Diabetic nephropathy is a late complication of diabetes, occurring progressively in susceptible patients after 15-25 years (21, 108, 110, 111). Diabetic albuminuria is associated with histopathologic features such as thickening of the GBM and mesangial expansion. In humans the progression of nephropathy and decline in glomerular filtration rate (GFR) are well correlated with pathologic features such as glomerulosclerosis, arteriolar hyalinosis, and tubulointerstitial fibrosis (26, 103, 104). The risk of nephropathy and progression is similar in type I and type II diabetes (63). Diabetic nephropathy is the leading cause of chronic kidney disease and about 40% of patients with end stage renal disease (ESRD) have diabetes (115). Diabetic nephropathy can be divided into five stages, see Figure 4 (111, 151). Stage 1 is characterized by a 30-40% increase in GFR above normal and occurs at the

onset of the disease. Insulin therapy does not normalize the GFR instantly, but rather within several weeks to a few months. The hyperfiltration is associated with enlarged kidneys and increased intraglomerular pressure, which may cause a transient increase in albumin excretion. Stage 2 is characterized by normal excretion of albumin (<30 mg/24 h) regardless of the duration of disease. Some patients maintain their hyperfiltration but patients with good diabetic control usually return to normal GFR (111). Stage 3, or incipient diabetic nephropathy, is characterized by microalbuminuria (30-300 mg/24 h) at rest, while patients with more marked albuminuria (101-300 mg/24 h) show a significant reduction in GFR (37). This suggests that the GFR begins to decline during the incipient stage of diabetic nephropathy. Blood pressure is often higher than in nondiabetic patients at this stage, though still in the normal range. Control of glucose levels and blood pressure, especially with angiotensin-converting enzyme inhibitors (ACEi) and/or angiotensin receptor blockers (ARB), reduces or eliminates microalbuminuria (44, 177).

With strict diabetic control, less than 20% of patient with type I diabetes and microalbuminuria progressed to overt nephropathy in a 10-year period (11). Instead, the majority reverted to normoalbuminuria. This is very encouraging because patients with normal albumin excretion rates maintained normal GFR and blood pressure even after 20 years of follow-up (44). Stage 4, or overt diabetic nephropathy, is characterized by clinical proteinuria (<0.5 g protein/24 h or <0.3 g albumin/24 h). Overt diabetic nephropathy develops in approximately 30-40% of patients with type I diabetes (44, 138). Recently, when patients were kept in strict diabetic control, less than 10% did so (10). Early at stage 4 the GFR may be in the normal range, but usually declines slowly and steadily. Also, blood pressure increases, and hypertension eventually occurs in almost all patients. Aggressive treatment of elevated blood pressure slows the rate of decline in GFR (108, 109, 114). At this point, aggressive treatment of elevated glucose concentrations has little effect. Once the process of nephron destruction is under way, it seems to proceed independently of cause, although lowering the blood pressure definitely helps. Stage 5, or ESRD, is similar to kidney failure resulting from any other cause. Diabetic patients undergoing dialysis have a poorer prognosis than nondiabetic patients. For this reason, kidney transplantation is considered the preferred method of treatment, especially if a

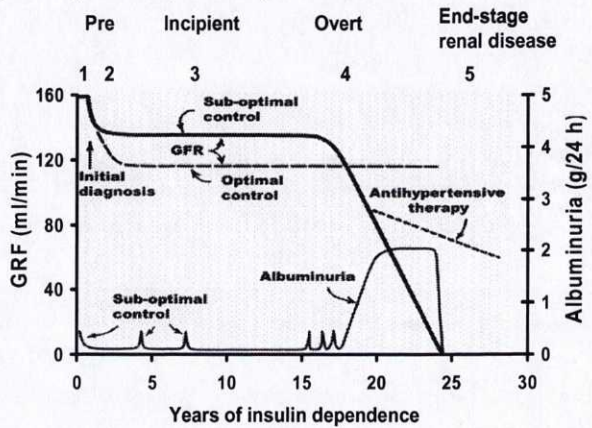


Figure 4. The changes in glomerular filtration rate (GFR) and albumin excretion in the progression of diabetic nephropathy. Modified from (71)

close relative can donate a kidney. Despite successful treatment for ESRD, many of these patients succumb to their associated cardiovascular disease.

Animal models of diabetic nephropathy

A pivotal criterion when using animal models in any pathophysiological research is to have close similarity between the pathological development in the animal and the corresponding patient. The major issue in animal models of diabetic nephropathy is the absence of ESRD. Whether this depends on an inadequate study period or a resistance to diabetic nephropathy remains uncertain. Below, some mouse models of diabetic nephropathy are discussed. The models mentioned here, and others, are carefully reviewed in a recent paper (18).

Streptozotocin is widely used to induce diabetes type I in mice (70, 91, 92, 159, 181). The advantages are that it is well established, has reproducible timing, and can be established in several strains. On the negative side are the potential for nonspecific toxicity, variable effects on the insulin production, and the strain dependent dosage. Another model for type I diabetes is the Ins2 Akita mouse with an autosomal dominant mutation (102, 173, 185). So far this model is only commercially available on a C57BL/6 background, a strain that is relatively resistant to diabetic nephropathy. The model used in this thesis, the non obese diabetic (NOD) mouse, spontaneously develops diabetes type I and have been widely used (45, 64, 88, 99, 150, 178, 187). The characteristics of the autoimmune disease contributing to the pancreatic β -cell destruction have been studied extensively, and the NOD mouse has a number of similarities with human type 1 diabetes (4, 20, 93). Disadvantages with this strain are the unpredictable timing of diabetic onset, the absence of an appropriate control strain, and the need for insulin therapy in longer studies.

Models of type II diabetes are for example, the Db/Db mouse and the Ob/Ob mouse. The Db/Db mouse has an autosomal recessive mutation in the leptin receptor (152) and the Ob/Ob mouse in the leptin (29). On a C57BLKS/J background the db/db mutation gives a more severe diabetic phenotype than on a C57BL/6 background. In humans, however, both of these mutations are very rare causes of diabetes type II. Another model of type 2 diabetes is the KK/ A^y mouse, which is produced by the transfer of the yellow obesity gene (A^y) into the inbred KK mouse. The mice have a complex phenotype of obesity and insulin resistance resulting in renal injury with significant albuminuria (117, 122).

AIMS

The general aim of this thesis was to evaluate macromolecular transport across the glomerular barrier under physiological and pathophysiological conditions.

The specific aims were:

- I. To develop a method for evaluation of glomerular size and charge selectivity in mice.

To develop a theoretical model describing the barrier as a gel of negatively charged fibers creating size and charge selectivity.

To investigate the charge and size selective properties of the barrier after digestion of the endothelial cell glycocalyx.
- II. To correlate a morphological change in the glomerular endothelial cell glycocalyx to a functional change of the barrier.
- III. To investigate functional, molecular and morphology changes of the glomerular barrier in long term diabetes.

MATERIALS AND METHODS

Animals

In paper I and II, experiments were performed on female C57BL/6jbm and C57BL/g mice, respectively. In paper III, female mice of the non-obese diabetic (NOD) strain (M&B, Stensved, Denmark) were used. The NOD mouse is a strain that spontaneously develops diabetes type I (see Introduction). Diabetic mice received insulin implants approximately every third week to maintain their blood glucose between 20-33 mmol/L. All mice were kept on standard chow and had free access to water. Experiments were approved by the Local Ethics Committee in Göteborg.

Anesthesia

Anesthesia was induced and maintained by inhalation of isoflurane (2-3% v/v) mixed with air (~1 L/min) in an isoflurane vaporizer. The body temperature of the mouse was kept at 37°C by means of a thermostatically controlled heating pad and a lamp connected to a temperature sensitive rectal probe.

Enzymes (papers I & II)

In Figure 5 a schematic diagram is shown outlining the proposed action of GAG degrading enzymes on endothelial cell glycocalyx. Enzyme dissolved in saline or saline alone (controls) was given as a bolus dose via the carotid artery (paper I) or the jugular vein (paper II). Doses and incubation times for all experiments are summarized in Table 1. Bovine testis hyaluronidase (E.C. 3.2.1.35, H3506, Sigma-Aldrich, Stockholm, Sweden) with a molecular weight of 56 kDa (pI: 6.6*) acts on glycosidic bonds in hyaluronic acid, dermatan, chondroitin, and chondroitin sulfate. Heparinase III from *Flavobacterium heparinum*, (E.C. 4.2.2.8, H8891, Sigma-Aldrich, Stockholm,

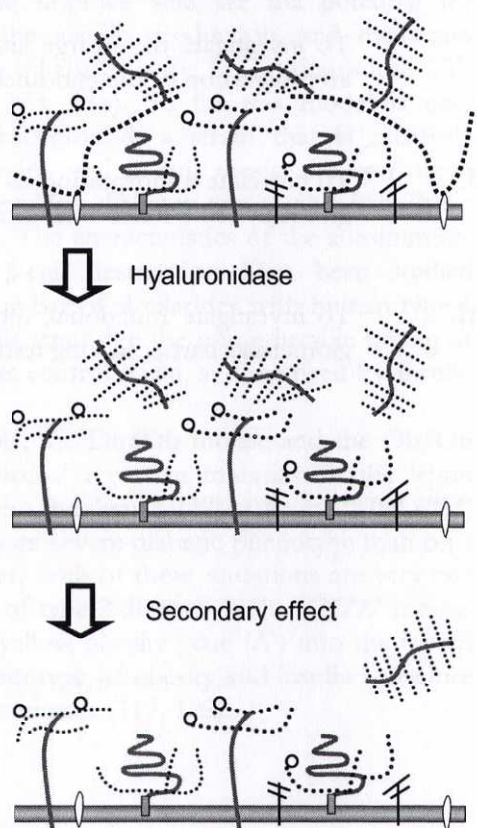


Figure 5. A schematic diagram of the proposed action of GAG digestion with hyaluronidase. See figure 3 for details regarding symbols.

Sweden) is a 70.8 kDa (pI: 7.9) enzyme that acts on heparan sulfate. Chondroitinase ABC from *Proteus vulgaris* (E.C. 4.2.2.4, C2905, Sigma-Aldrich, Stockholm, Sweden) has a molecular weight of approximately 120 kDa (pI: 7.4*). This enzyme acts on chondroitin 4-sulfate, chondroitin 6-sulfate, dermatan sulfate, and slowly on hyaluronic acid.

* estimated from Swiss-Prot/TrEMBL

Table 1. Enzyme doses and incubation time for the experiments.

Group	Enzyme	Dose (U/kg)	Incubation (min)	Experiment
Control 1	Saline		15, 60	cIPK (I), in vivo (I)
Control 2	Saline		15	cIPK (II), EM (II)
Hya	Hyaluronidase	15·10 ³	60	cIPK (I), in vivo (I), EM (II)
Hep LD	Heparinase III	8.2	60	cIPK (I), in vivo (I)
Hep HD	Heparinase III	82	15	cIPK (I), in vivo (I), EM (II)
Chond LD	Chondroitinase	87	15	cIPK (II), EM (II)
Chond HD	Chondroitinase	435	15	cIPK (II), EM (II)

cIPK – cooled isolated perfused kidney, EM – electron microscopy with Intralipid® droplets

Tail-cuff plethysmography (paper III)

The tail-cuff method was used for non-invasive measurements of systolic blood pressure in paper III. Measurements were repeated for at least 8 times on 2 consecutive days every third week in diabetic animals. The tail-cuff system lacks the precision and sensitivity of systems that directly measure intra-arterial pressure, but its reliability and reproducibility are well documented (86, 87)

Glomerular barrier studies

Tracers (papers I-III)

⁵¹Cr-EDTA was used for determination of the glomerular filtration rate (GFR). This solute is small, freely filtered, and not reabsorbed or secreted. Human serum albumin (HSA) has a molecular weight of 68 kDa and a Stokes-Einstein radius of 35.5 Å. The net surface charge of albumin is -23 (51). Ficolls are inert sucrose polymers that have a net surface charge of zero and are considered to be spherical. The Ficolls come in a molecular size range of 12-70 Å.

In vivo (paper I)

The jugular vein was cannulated (PE-25) to serve as a route for infusion of tracer solution at a rate of 0.7 ml/h by a syringe pump (Razel Scientific instruments inc., Stanford, USA). The tracer solution was composed as follows: 3 MBq/L ⁵¹Cr-EDTA, 1.5 MBq/L ¹²⁵I-labeled human serum albumin (HAS, IT.20S; Isopharma AS, Kjeller, Norway), 3 g/L FITC-Ficoll, 83 mM glucose, 30 mM bicarbonate, and 205 mM saline. ¹²⁵I-HAS was filtered through an equilibrated desalting column (Sephadex G-25 PD-10, Amersham Pharmacia Biotech, Uppsala, Sweden) to remove the free iodine content before it was added to the tracer solution. Infusion

of tracer solution was started 30 minutes prior to sample collections. An injection of furosemide (2 mg/kg, Benzon Pharma A/S, København, Denmark) was given 5 minutes before the first urine collection. Blood samples were aspirated from the carotid artery with 10 minute intervals, urine was collected between each of the three blood samples, allowing estimations of GFR and fractional clearances for Ficolls and albumin.

The cooled isolated perfused kidney model, cIPK (papers I-III)

The cIPK model (Figure 6) allows estimation of the glomerular barrier without the tubular modifications of primary urine that occurs *in vivo*. The mouse was eviscerated and the intestines removed. The aorta and caval vein were freed from surrounding tissue and clamped distal to the renal arteries.

The aorta was cannulated in retrograde direction with a T-tube (PE-25), connected to a pressure transducer, a few millimeters distal to the clamp. The clamp was removed, allowing perfusion of the kidneys by means of a pulsatile pump (Ismatec IPC, Zurich, Switzerland). The aorta was then ligated proximal to the renal arteries, and the caval vein was opened distal to the renal arteries for venous outflow. After a short period of equilibration, urine samples were collected and weighed. Perfusion pressure and urine weight changes were monitored by a computer using AcqKnowledge v 3.7.3 (Biopac Systems Inc, Goleta, CA) computer software. Care was taken not to touch the kidneys and to provide adequate perfusion with either blood or perfusate during the preparation procedure. The temperature of the perfusate was maintained at 8°C in order to inhibit tubular function as well as energy consumption and myogenic tone (25, 47) without altering capillary permeability (121, 136).

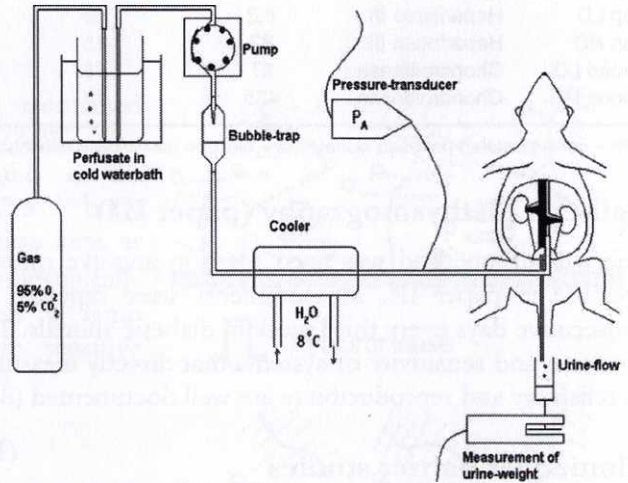


Figure 6. The cooled isolated perfused kidney model.

After a short period of equilibration, urine samples were collected and weighed. Perfusion pressure and urine weight changes were monitored by a computer using AcqKnowledge v 3.7.3 (Biopac Systems Inc, Goleta, CA) computer software. Care was taken not to touch the kidneys and to provide adequate perfusion with either blood or perfusate during the preparation procedure. The temperature of the perfusate was maintained at 8°C in order to inhibit tubular function as well as energy consumption and myogenic tone (25, 47) without altering capillary permeability (121, 136).

Perfusate (papers I-III)

Perfusate was prepared using a modified Tyrode solution with human serum albumin (HSA, 18 g/L, Immuno, Vienna, Austria) to which the tracers were added. The solution had the following composition: 113 mM NaCl, 4.3 mM KCl, 2.5 mM CaCl₂, 0.8 mM MgCl₂, 25.5 mM NaHCO₃, 0.5 mM NaH₂PO₄, 5.6 mM glucose, 0.9 mM nitroprusside (Merck, Darmstadt, Germany), 10 mg/L furosemide, 300 mg/L fluorescein isothiocyanate (FITC) labeled Ficoll (Bioflor HB, Uppsala, Sweden),

0.16 MBq/L ^{51}Cr -EDTA (Amersham Pharmacia Biotech, Buckinghamshire, UK). All solutions were made with fresh distilled water with a resistivity of 18.2 M Ω /cm. The perfusate (pH 7.4) was protected from light and gassed with 5% CO₂ in O₂.

Data analysis (papers I-III)

Perfusate, plasma and urine samples were analyzed for ^{51}Cr -EDTA, plasma and urine samples also for ^{125}I -HAS, using a gamma-counter (Cobra, AutoGamma Counting systems, Packard Instrument Company, Meridian, CT, USA). Data was used for later calculations of GFR and fractional clearances for albumin (see Calculations). Corrections were made for background activity and ^{51}Cr -EDTA spillover. In addition, the albumin concentration of all urine samples from the cPKs was determined by radioimmunoassay (Pharmacia and Upjohn Diagnostics Sverige AB, Uppsala, Sweden).

Analysis of Ficoll (papers I-III)

The fractional clearance for different radii of FITC-Ficoll was calculated by subjecting perfusate, plasma, and urine samples to gel filtration and detection of fluorescence (Dionex fluorimeter RF-2000 Dionex Softron, Gynkotek, Germering, Germany) using Chromeleon (Gynkotek, Germering, Germany) software. A 0.05 M phosphate buffer with 0.15 M NaCl, pH 7.0, was used as eluent. A volume of 5 μl from each sample was analyzed at an excitation wavelength of 492 nm and an emission wavelength of 520 nm (paper I) or 560 nm (paper II, III). The flow rate and the sampling frequency (1 per second) were maintained constant during the analysis and so were pressure and temperature (8°C). For details regarding calculation of fractional clearances see Calculations.

Models of the Glomerular Barrier

The heterogeneous charged fiber model (paper I)

There have been few attempts to combine the estimation of size and charge selectivity in one model, due to the complex equations involved. We have developed a heterogeneous charged fiber model by applying a theoretical model of the distribution of charged and neutral solutes in charged gels (77) to the settings of glomerular filtration. Johnson and Deen (77) extended the partition theory by Ogston (118), predicting the concentration ratio of a solute at equilibrium in and outside a gel by a Boltzmann factor. By this, they obtained partition coefficients for neutral and charged solutes in charge fiber gels. We extended their work and estimated reflection coefficients, restriction for diffusion, and clearance from these partition coefficients.

The endothelial glycocalyx could be considered as such a charged fiber gel, where GAG chains alone or on proteoglycans form an aqueous fiber matrix or gel structure. The glomerular basement membrane is another charged gel. We have previously used the model in a quantitative analysis of charge-selectivity (163), but the present analysis differs in one important aspect, namely the introduction of

heterogeneous fiber densities, i.e. a shunt pathway or large pores. Basically, the important parameters in the model are: the fiber radius (r_f), the relative concentration of fibers in the gel (ϕ), the surface charge densities of solute (q_s) and fiber (q_f), the unrestricted exchange area over diffusion distance (A_0/Δ_x), and the large pore radius (r_l). By using nonlinear regression analysis, the model parameters are fitted to the experimental fractional clearances for albumin and the neutral Ficolls of different radii. We assumed the fiber radius (r_f) to be 5 Å and the solute (albumin) radius (r_s) to be 35.5 Å, and the surface charge densities (q) of fiber, albumin, and Ficoll to be -0.2, -0.022, and 0 C/m², respectively. For further details regarding calculations, please consult paper I.

The gel-membrane model (paper I-III)

According to the gel-membrane model (120), the glomerular barrier is composed of two separate compartments in series: one charge-selective (gel) and one size-selective (membrane). The gel is in contact with plasma and contains fixed negative charges that reduce the concentration of anionic solutes, such as albumin. The second compartment of the barrier behaves as a membrane exerting size selectivity but no charge selectivity. The concentration of solutes in the primary urine will depend on the effects of these two barrier components as outlined below. For calculations of charge-selectivity, the fractional clearances for albumin and its neutral counterpart of similar size, Ficoll 35.5Å, are compared giving an estimation of the charge density (ω) in the glomerular barrier. Size selective properties can be described using a two-pore model with experimental fractional clearance data for Ficolls of molecular radii ranging from 30-70 Å. In brief, the exchange can be described using the following parameters: the functional small pore radius (r_s), large pore radius (r_l), the large pore fraction of the glomerular filtrate (f_l), and the unrestricted exchange area over diffusion distance (A_0/Δ_x) (135). By using a nonlinear regression analysis and a previously defined set of physiological equations (120) model parameters are fitted to the experimental fractional clearances of neutral Ficoll of different radii. Nonlinear flux equations are used to calculate the net fluxes of fluid and solutes for each pore pathway, individually (135). For further details regarding calculations, please consult Ohlson et al (120).

Lognormal distribution + shunt model (paper I)

Experimental fractional clearance data for Ficolls with molecular radii ranging from 30-70 Å can also be described using a lognormal distribution + shunt model (41, 123). In this model the glomerular barrier is considered to have many pores with radii that obey a lognormal probability distribution together with a few non-selective shunts. The parameters to determine in the model are, mean pore radius, the width of the lognormal distribution, the large pore fraction of the glomerular filtrate (f_l), and the unrestricted exchange area over diffusion distance (A_0/Δ_x). The shunt was set to 150 Å, since a non-selective or higher shunt radius gave a poor fit for large solutes.

Glomerular morphology

General morphology (paper I)

To ensure that the enzymes did not destroy the ultra-structure of the glomerular filtration barrier, i.e. endothelial cells, glomerular basement membrane, and podocytes, electron microscopy was used. Under anaesthesia, controls and mice treated with hyaluronidase ($15 \cdot 10^3$ U/kg for 60 min) or heparinase (82 U/kg for 15 min) were perfused at 100 mmHg intracardially with Tyrode-buffer containing 1 mg/ml xylocain followed by fixative, 2.5% glutaraldehyde in 0.05 M Na-cacodylate (pH 7.2). The kidneys were removed, processed for electron microscopy, and examined in a Zeiss 902 electron microscope.

Glycocalyx estimation (paper II)

The effect of the enzymes on endothelial cell glycocalyx was estimated by the use of an indirect marker, Intralipid[®]. Intralipid[®] (Pharmacia & Upjohn Sverige AB, Stockholm, Sweden) was prepared by discarding the top lipid layer after a night in refrigerator. An enriched floating fraction of lipid droplets was obtained after centrifugation at $3000 \times g$ for 10 minutes, and 100 μ l was administered into the caval vein. After allowing mixing in the circulation for 10 minutes the left renal artery and vein were clamped and the kidney was fixed by subcapsular injection of Karnovsky's fixative (2.5% paraformaldehyde and 2% glutaraldehyde in 0.05 M Na-cacodylate buffer, pH 7.2). The kidneys were removed, processed for electron microscopy, and examined in a Leo 912AB Omega electron microscope (Leo Electron Microscopy Ltd., Cambridge, England). Micrographs at a magnification of 8000 were obtained from 4-7 animals in each group giving a total of 624 glomerular capillaries for the measurements. For each micrograph the distance between the Intralipid[®] droplets and the luminal cell surface of the endothelium was measured in the zone 0-500 nm from the endothelium using EsiVision Pro (Soft Imagine System GmbH, Münster, Germany) computer software. In total, the distance for ~3200 droplets was measured. For the sake of simplicity, the relative frequency of droplets for each of a series of 50 nm increment zones was calculated.

Glomerular basement membrane thickness (paper III)

The kidney was fixed by subcapsular injection of Karnovsky's fixative (2.5% paraformaldehyde and 2% glutaraldehyde in 0.05 M Na-cacodylate buffer, pH 7.2). The kidneys were removed, processed for electron microscopy, and examined in a Leo 912AB Omega electron microscope (Leo Electron Microscopy Ltd., Cambridge, England). Glomerular basement membrane thickness was measured in electron micrographs where the thickness was defined as the distance between the podocyte foot process and the corresponding endothelial cell. To ensure proper cross-sectioning, a slit diaphragm between the foot-processes had to be visible, as well as, a single layer of endothelial cells.

Glomerular size and sclerosis (paper III)

Sclerotic areas were visualized with periodic acid Schiff's (PAS) staining on 4 μm cryosections. Tissue sections were examined in light microscopy at 40x magnification. The glomerular and sclerotic areas were estimated using quantitative software, see example in Figure 7.

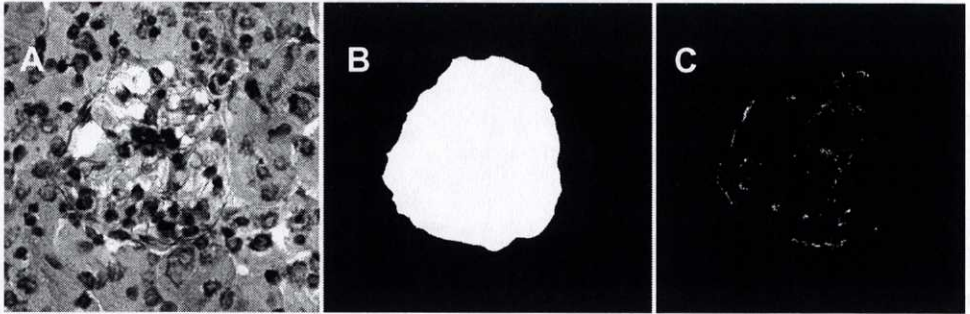


Figure 7. Estimation of glomerular surface area and sclerotic area. In PAS-stained tissue the glomeruli (A) interface was marked (B) as well as sclerotic areas (C).

Protein and mRNA expression (paper III)

Quantitative Real-time PCR

RNA was prepared from fresh frozen renal cortex using the Qiagen mini kit (Roche Diagnostics, Bromma, Sweden). The concentration and quality of the RNA was determined by the Agilent 2100 bioanalyzer, see example in Figure 8 (Nano LabChip, Agilent Technologies, Waldbronn, Germany). Synthesis of cDNA was carried out using 1 μg of the RNA in an avian myeloblastosis virus reverse transcriptase (AMV RT) buffer with AMV RT, dNTP (deoxy-CTP, -GTP, -TTP and -ATP), random hexamers, and RNase inhibitor (all reagents from Roche Diagnostics, Bromma, Sweden) in a final volume of 20 μl . The reaction conditions were 5 min at 25°C, 50 min at 42°C followed by 5 minutes at 70°C. The mRNA level of each target gene was quantified by real-time PCR on the ABI Prism 7900 Sequence Detection system (Taqman, Applied Biosystems Inc., Foster City, CA) using the Low Density Array (LDA). For example of an amplification plot, see Figure 9. The LDA can detect 23 genes in duplicates in one run, including endogenous controls, and was designed with primer and probes for the genes summarized in Table 2. The PCR was carried out in a reaction mix containing 50 ng sample cDNA and Taqman universal PCR master mix (ABI; containing MgCl_2 , dUTP, dATP, dCTP, dGTP, Taq Gold polymerase, and AmpEraseUNG). The AmpEraseUNG was activated before the denaturing step by heating for 2 min at 50°C. Samples were denatured at 95°C for 10 min and then subjected to 40 cycles of 2-step PCR, 15 sec at 96°C and 1 min at 60°C. All samples were corrected for an average of the endogenous controls 18S and β -actin. Also, they were run twice giving a mean from 4 reactions in total for each gene.

Table 2. Genes targeted by real-time PCR

Protein	Accession No.	Protein description	Change compared to Control	
			D10	D40
18S		Endogenous control		
β -actin	NM_007393	Endogenous control		
Biglycan	NM_007542	CS/DS, SLRP, secreted	-	↓
Decorin	NM_007833	CS/DS, SLRP, secreted	-	↓
Fibromodulin	NM_021355	KS, SLRP, secreted	-	-
Versican	D28599	CS, secreted	-	↓
Perlecan	M77174	HS/CSPG, secreted	-	-
Glypican-1	NM_016696	HSPG, GPI-anchored	-	-
Glypican-4	NM_008150	HSPG, GPI-anchored	-	-
Syndecan-1	NM_011519	HSPG, membrane bound	-	-
Syndecan-4	NM_011521	HSPG, membrane bound	-	-
Nephrin	NM_019459	Podocyte slit	-	-
Podocin	NM_130456	Podocyte slit	-	↓
PKC δ	NM_011103	Protein kinase C	-	-
MMP-9	NM_013599	Matrix metalloprotease-9	-	↓

CS-chondroitin sulfate; DS-dermatan sulfate; SLRP-small leucine rich proteoglycan; KS-keratan sulfate; HS-heparan sulfate; PG-proteoglycan; GPI-glycosyl phosphatidylinositol; down-regulated expression (↓) and unchanged expression (-) compared to control

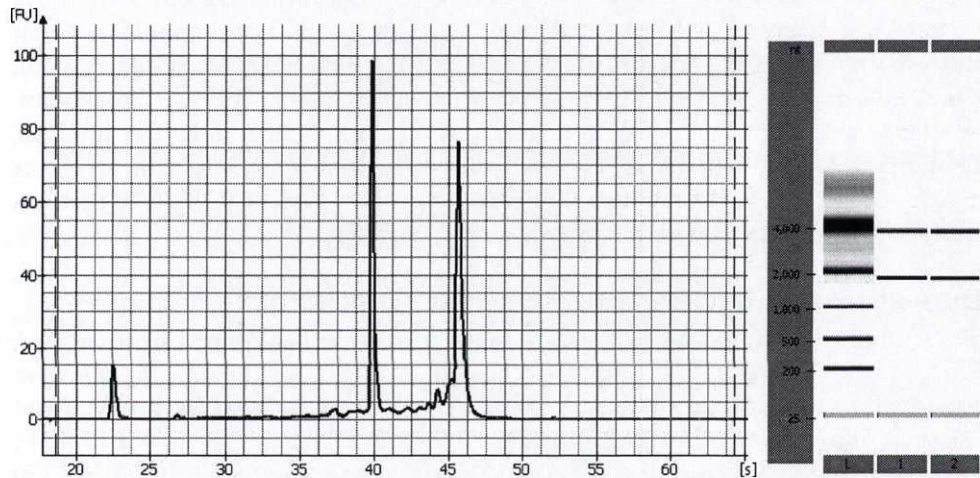


Figure 8. Example of a RNA sample after running the Agilent NanoChip[®]. The two peaks correspond to ribosomal 18S (40 s) and 28S (46 s), while the small peak seen at 23 s is a marker. On the right is a gel picture showing the two ribosomal bands in duplicate (1 and 2) and the ladder (L).

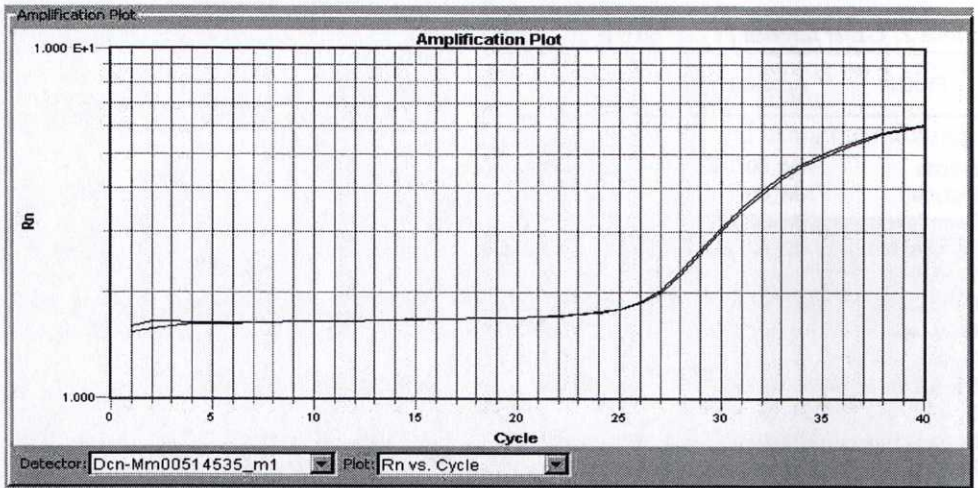


Figure 9. Amplification plot of sample cDNA analyzed by real-time PCR run in duplicate.

Immunohistochemistry

Immunohistochemistry was performed to analyze the expression of different proteins on 4 μm fresh frozen tissue sections. Sections were blocked with 100% FCS (fetal calf serum) and incubated with the following primary antibodies: rabbit anti-versican antibody (2 $\mu\text{g}/\text{ml}$, 1 h at RT; Affinity BioReagents, Golden, CO), rabbit anti-podocin antibody (0.5 $\mu\text{g}/\text{ml}$, 1 h at RT, Sigma-Aldrich, Stockholm, Sweden), and rabbit anti-decorin antibody (2 $\mu\text{g}/\text{ml}$, 1 h at RT; Abcam Ltd., Cambridge, UK). After rinsing, the sections were incubated 1 h with an Alexa conjugated goat anti-rabbit antibody (Molecular probes, Eugene, OR). The sections were mounted and evaluated by fluorescence microscopy.

Western blot

The protein concentrations in renal cortex lysates were determined using a BCA Protein Assay Reagent kit (Pierce, Rockford, IL). Protein lysates (5 μg) were separated on NuPAGE precast 4-12% Bis-Tris gels (Novex, San Diego, CA). After electrophoresis the proteins were transferred to polyvinylidene difluoride (PVDF) membranes. Membranes were blocked with 5% non-fat dry milk in TBS-T (30 mM Tris-HCl pH 7.5, 100 mM NaCl, and 0.1% Tween 20). Membranes were incubated with rabbit anti-decorin antibody (2 $\mu\text{g}/\text{ml}$, 1 h at RT; Abcam Ltd., Cambridge, UK). After rinsing, the membrane was incubated with horseradish peroxidase (HRP)-conjugated anti-rabbit antibody (Amersham Life Science, Amersham, UK). Immunoreactive bands were visualized using enhanced chemiluminescence (ECL plus, Amersham Biosciences, Uppsala, Sweden) and a CCD camera (LAS1000, Fujifilm, Tokyo, Japan).

Calculations

Glomerular filtration rate (GFR)

GFR was calculated from the urine over plasma concentration ratios (C_U/C_P), determined by ^{51}Cr -EDTA times urine flow (Q_U) according to the equation:

$$\text{GFR} = \left(\frac{C_U}{C_P} \right)_{\text{Cr-EDTA}} \cdot Q_U \quad (\text{Eq. 1})$$

Fractional clearance, θ

The renal clearance (Cl) of a solute X can be calculated from the amount excreted in the urine (C_U) over the plasma concentration (C_P) during a certain period of time according to the equation: $\text{Cl} = (C_U/C_P)_X \cdot Q_U$. The fractional clearance (θ) of a solute is given by its Cl over GFR. Thus, combining Eq.1 with the Cl equation above yields:

$$\theta_X = \frac{\left(\frac{C_U}{C_P} \right)_X}{\left(\frac{C_U}{C_P} \right)_{\text{Cr-EDTA}}} \quad (\text{Eq. 2})$$

Quantification of mRNA

Gene expression differences between controls (C) and diabetic animals (D10 and D40) were estimated using the comparative $\Delta\Delta C_T$ method of relative quantification. Correcting the gene expression for the endogenous control (e) yields:

$$X_G = K(1 + E)^{-\Delta C_{T(e)}} \quad (\text{Eq. 3})$$

where X_G is the normalized amount of expression, K a constant, E the efficiency, and ΔC_T the difference in threshold cycle for the gene of interest and the endogenous control. Using the normalized gene expression from one control and dividing all other expressions with that yields:

$$\frac{X_G}{X_C} = \frac{K(1 + E)^{-\Delta C_{T(e)}}}{K(1 + E)^{-\Delta C_{T(e)}}} = (1 + E)^{-\Delta\Delta C_T} \quad (\text{Eq. 4})$$

where X_G and X_C are the gene expression for a sample and C a reference or control sample, respectively. Furthermore,

$$\Delta\Delta C_T = \Delta C_{T(G)} - \Delta C_{T(C)} \quad (\text{Eq. 5})$$

For the low density array the efficiency is close to 1, and thus the relative quantification RQ, normalized to endogenous control and related to a control sample is given by:

$$\text{RQ} = 2^{-\Delta\Delta C_T} \quad (\text{Eq. 6})$$

This will give a relative quantification for all gene expressions compared to one control thus giving a distribution of gene expressions in all groups used in the statistical comparisons. In addition, we performed normalizations for both the endogenous controls 18S and β -actin when calculating the relative quantification.

Statistics

Results are presented as means with 95% confidence intervals (paper I) or as means \pm SEM (papers II & III). In this thesis all results are presented as means \pm SEM. In all papers, statistical comparisons were made using one-way analysis of variance (ANOVA), with post hoc Games-Howell to test for significant differences. In the case of uneven distribution the statistical analysis was based on logarithmic values. A p-value less than 0.05 was considered statistically significant.

REVIEW OF RESULTS

The cIPK model versus in vivo

Experiments were performed in vivo (paper I) or using the cIPK (paper I-III). Control 1 and control 2 are the cIPK controls from paper I and II, respectively. The fractional clearance for albumin was underestimated by one order of magnitude in vivo as a result of significant tubular reabsorption and degradation of albumin compared to the cIPK (Figure 10). The fractional clearance for Ficoll 35.5 Å, the neutral counterpart of albumin, was similar both in vivo and in the cIPK controls. As expected, GFR was lower in the cIPK than in vivo ($p < 0.001$, Figure 11).

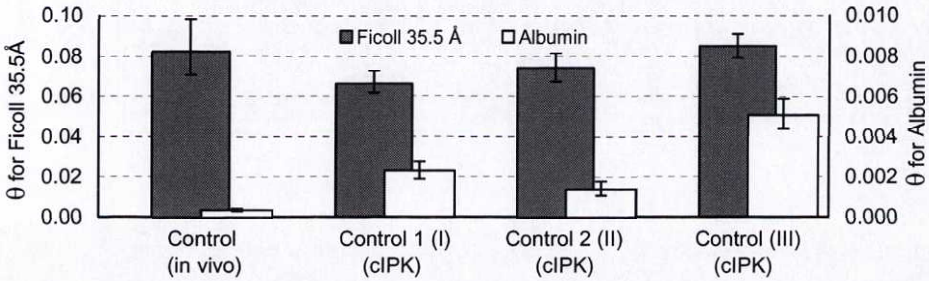


Figure 10. Mean \pm SEM of the fractional clearance (θ) for albumin and Ficoll 35.5, the neutral counterpart of albumin, in controls from all experimental groups. Please note that they are plotted on different scales.

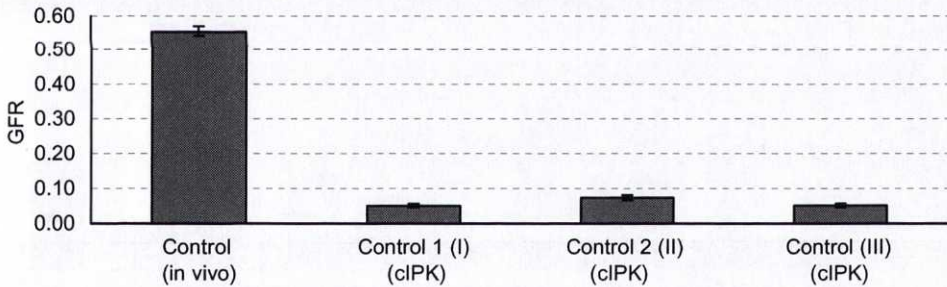


Figure 11. Glomerular filtration rate (GFR) for control groups in vivo and in the cIPK

Endothelial cell glycocalyx in the glomerular barrier (paper I, II)

Functional aspects

The isolated perfused kidneys at 8°C revealed that the fractional clearance for albumin was significantly increased up to 5-fold after treatment with hyaluronidase or the high dose of chondroitinase ($p < 0.05$ and $p < 0.001$, respectively, Figure 12). The fractional clearance for Ficoll 35.5 Å, the neutral counterpart of albumin, was similar in all groups.

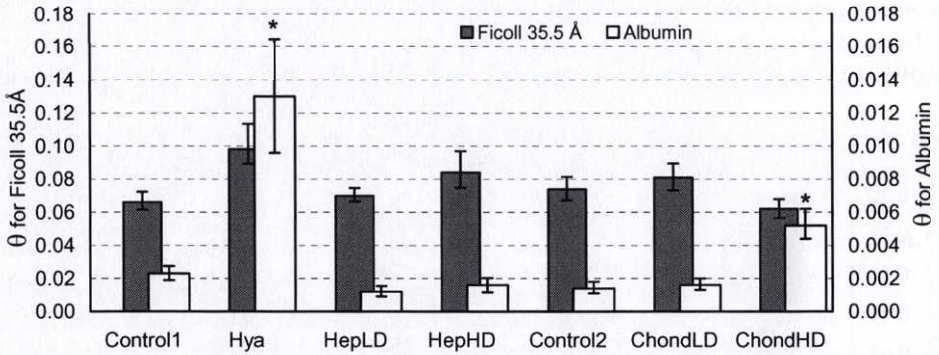


Figure 12. Mean \pm SEM of fractional clearance (θ) for the neutral Ficoll 35.5 Å and the negatively charged albumin. Please note that they are plotted on different scales. (*) denotes a significant difference compared to respective control.

Estimations of charge and size selectivity were performed using mathematical models of the glomerular barrier. The heterogeneous charged fiber model in paper I and the gel-membrane model with two-pore analysis in paper II showed that size selectivity of the glomerular barrier was unaltered by all enzyme treatments (Figure 13). The same models revealed that hyaluronidase or the high doses of heparinase or chondroitinase gave a decreased fraction of negatively charge fibers (paper I) or a decreased charge density (paper II) in the glomerular barrier (Figure 14).

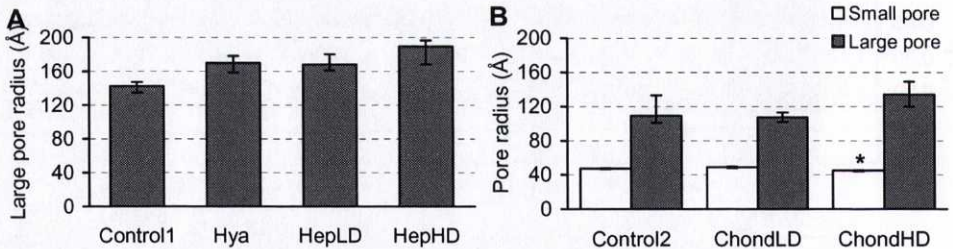


Figure 13. Mean \pm SEM for the large pore radius in paper I (A) and the small and large pore radii in paper II (B). (*) denotes a significant difference compared to respective control.

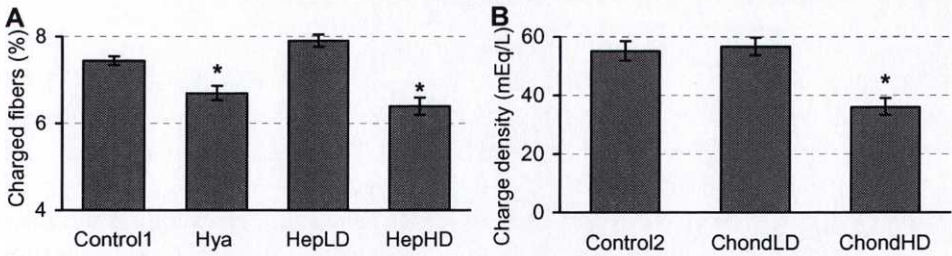


Figure 14. Mean \pm SEM of the negatively charged fiber fraction in paper I (A) and the negative charge density in paper II (B) in the glomerular barrier. (*) denotes a significant difference compared to respective control.

Morphological aspects

The thickness of the endothelial cell glycocalyx was measured indirectly using the distance between Intralipid[®] droplets and the luminal plasma membrane of the endothelium in flow-arrested and fixed kidneys. The evaluation of micrographs (Figure 15) revealed that digestion with either enzyme i.e. hyaluronidase, heparinase or chondroitinase, gave a significant increase in the relative frequency of Intralipid[®] droplets in the zone closest to the endothelium (Figure 16).

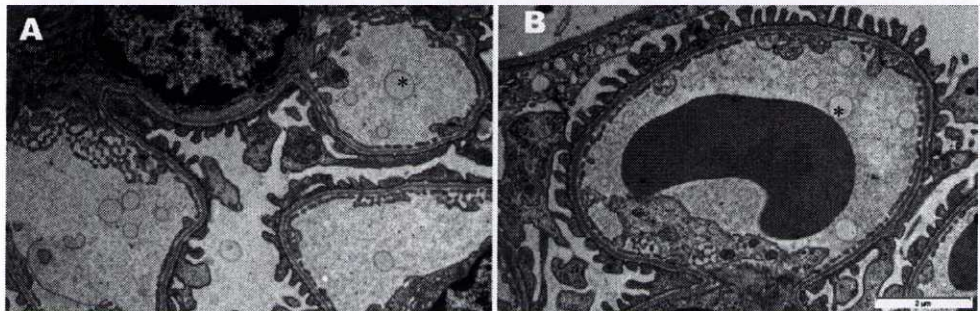


Figure 15. Glomerular capillaries with Intralipid[®] droplets (*) from a control (A) and a heparinase treated animal (B).

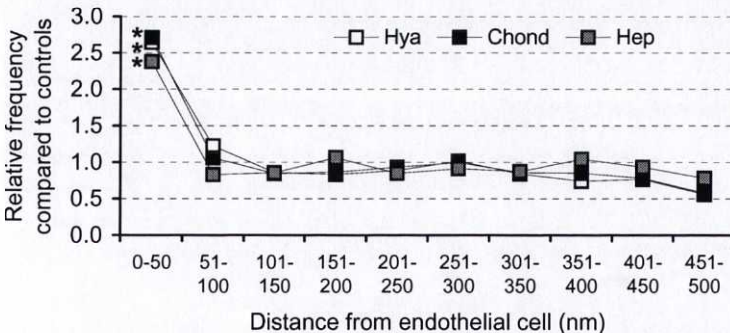


Figure 16. The increase in relative frequency of Intralipid droplets. (*) denotes a significant difference compared to control.

The Glomerular Barrier in Diabetes (paper III)

Diabetic Nephropathy in the NOD mouse

Diabetic mice showed a significant ($p < 0.001$) increase in glomerular area and PAS positive staining as estimated with light microscopy. Using transmission electron microscopy the glomerular basement membrane (GBM) was measured and found to be significantly ($p < 0.001$) increased in both diabetic groups. Also, a tendency of hyperfiltration was seen at 10 weeks of diabetes. Data regarding glomerular morphology and GFRs are shown in Figure 17 and 18. Systolic blood pressure remained constant during the 40 weeks of diabetes (Figure 19).

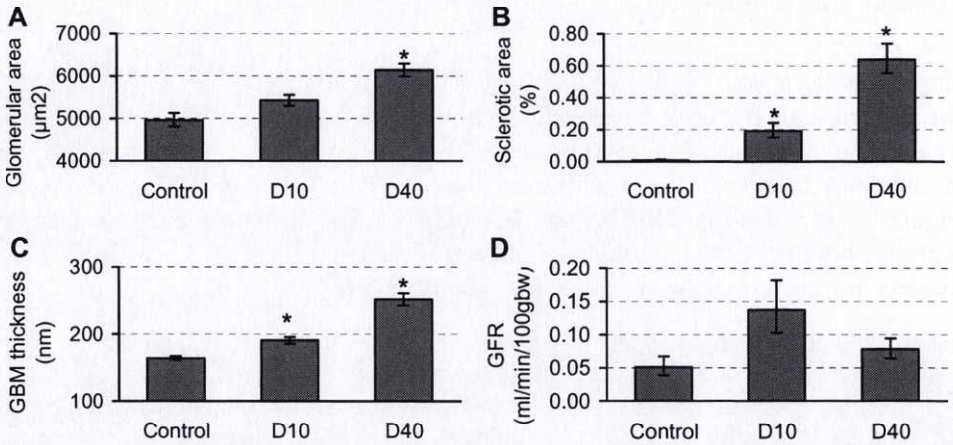


Figure 17. Mean \pm SEM of glomerular surface area (A), sclerotic area in glomeruli (B), GBM thickness (C) and GFR (D). (*) denotes a significant difference compared to controls.

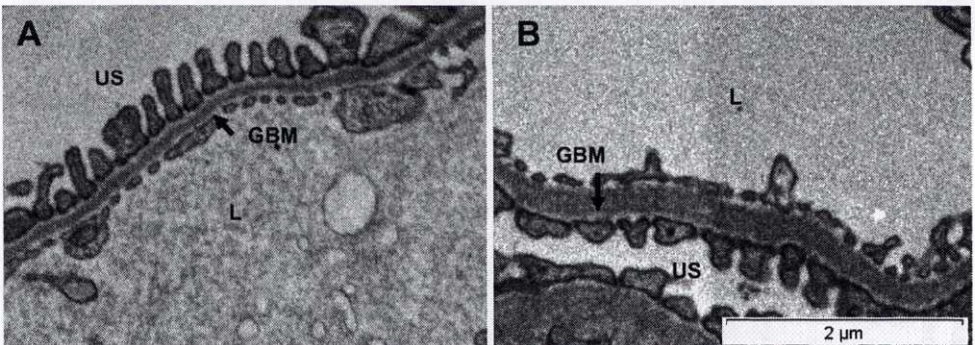


Figure 18. Electron micrographs of the glomerular barrier illustrating the glomerular basement membrane (GBM) in control (A) and after 40 weeks of diabetes (B). Capillary lumen (L), urinary space (US)

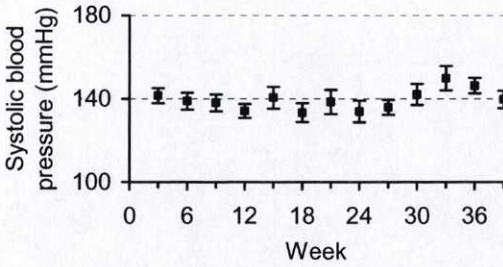


Figure 19. Mean \pm SEM of systolic blood pressure estimated with tail-cuff in diabetic mice.

Functional aspects

In vivo, albuminuria remained similar until week 24, whereafter a slight increase could be seen (Figure 20). Data from the cIPK showed that the fractional clearance for albumin was increased significantly ($p < 0.001$) after 40 weeks of diabetes (Figure 21). The fractional clearance for Ficoll 35.5 Å, the neutral counterpart of albumin, was similar in all groups with no significant differences. To further describe the glomerular barrier, mathematical estimations were done using the data above and the fractional clearances for all Ficoll sizes (12-70 Å) in a gel-membrane model, including two-pore analysis and calculations of charge density. The two-pore analysis showed no increase in small or large pore radius in diabetes, reflecting unaltered size selectivity (Figure 22). The radius was 46.2-46.8 Å for the small pore and 108-167 for the less frequent large pore. There was a reduction in charge density in the glomerular barrier from 41.0 mEq/L in controls to 25.1 mEq/L after 40 weeks of diabetes ($p < 0.01$, Figure 22).

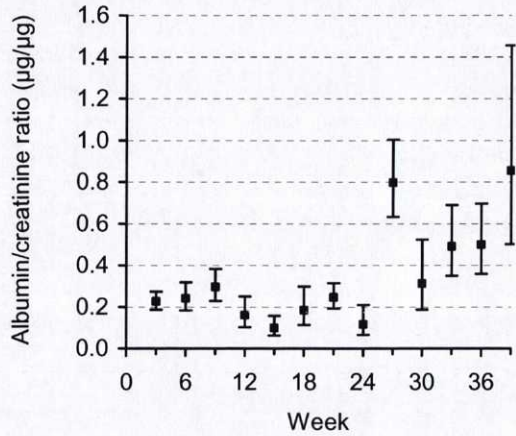


Figure 20. Mean \pm SEM of albumin to creatinine ratio for diabetic mice.

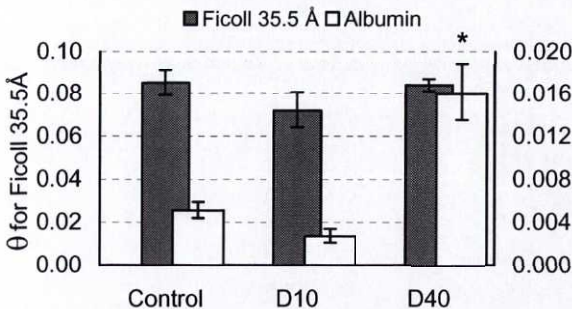


Figure 21. Mean \pm SEM of the fractional clearance for albumin and Ficoll 35.5 Å, the neutral counterpart of albumin. Please note that they are plotted on different axes. (*) denotes a significant difference compared to controls.

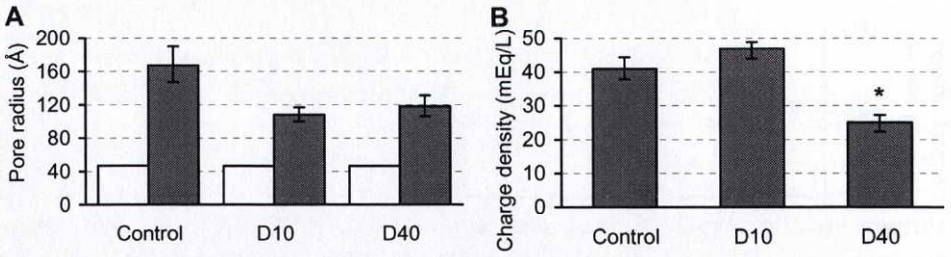


Figure 22. Mean \pm SEM of estimated size selectivity with the two-pore model (A) and charge selectivity illustrated as the charge density of the glomerular barrier (B). (*) denotes a significant difference compared to controls.

Molecular aspects

Real-time PCR revealed a significant down-regulation in renal cortex of several genes in diabetes compared to controls. After 40 weeks of diabetes mRNA expression for versican and matrix metalloprotease-9 was found to be down-regulated compared to control. Expression of mRNA for the small leucin rich proteoglycans biglycan, decorin, and the slit diaphragm podocin was down-regulated at week 40 as well (Figure 23, Table 2). Immunohistochemical localization of the core proteins of versican, podocin, and decorin together with a Western blot for decorin are shown in Figure 24.

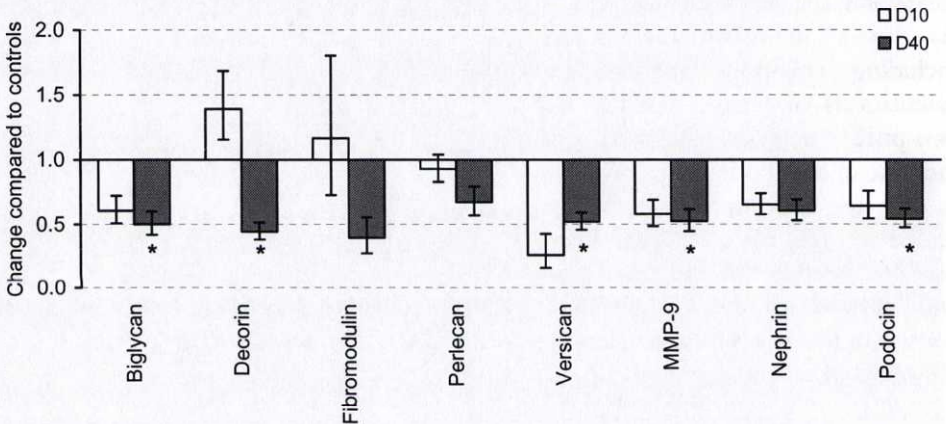


Figure 23. Mean \pm SEM of mRNA expression in renal cortex. (*) denotes a significant difference compared to control.

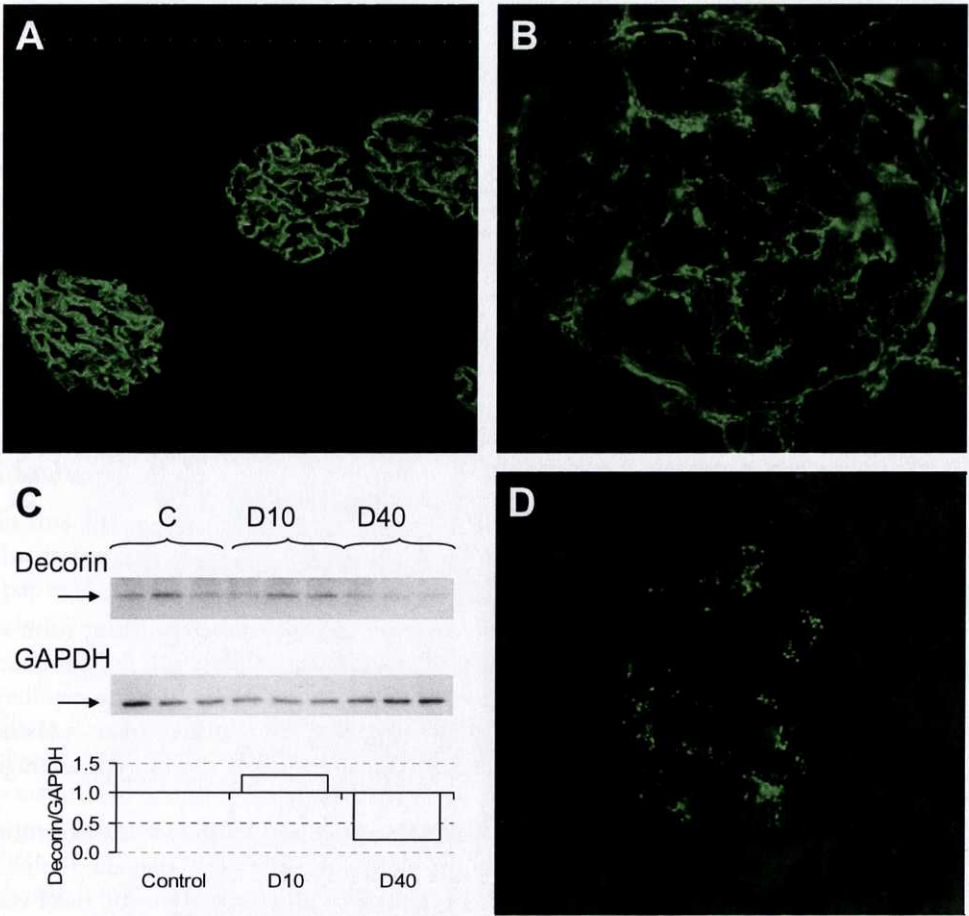


Figure 24. Immunohistochemical localization of proteins in glomeruli of control mice; podocin (A), versican (B), and decorin (D). In (C) a Western blot for decorin is shown. Staining for podocin was only found in the glomeruli, while decorin and versican also showed staining in some tubular structures.

DISCUSSION

This thesis is based on three papers that investigate the properties of the glomerular barrier in healthy and diabetic kidneys. In paper I and II the importance of the glomerular endothelial cell glycocalyx with respect to glomerular charge selectivity is studied. This thesis describe that altered morphology in the glycocalyx have a functional consequence, namely a decreased charge selectivity. Moreover, GAGs are the structures important for this feature. To further study the involvement of proteoglycans and their GAGs in disease, functional, morphological, and molecular alterations in diabetic nephropathy were investigated. Diabetic nephropathy is a complication of diabetes known to alter the glomerular barrier, hence causing albuminuria. However, the underlying mechanisms are unknown. This thesis show that albuminuria in diabetic nephropathy is due to altered charge selectivity. Also, the mRNA expressions of proteoglycans such as versican, biglycan, decorin together with MMP-9 and podocin are down-regulated in long term diabetes where albuminuria occurs.

In vivo versus the cIPK

The cIPK is a model where the glomerular barrier can be studied without tubular modifications of the primary urine. Cooling of the kidneys inhibits tubular function as well as energy consumption and myogenic tone (25, 47) without altering capillary permeability (121, 136). This is reflected by the low urine over plasma concentration for $^{51}\text{Cr-EDTA}$ (1.15) in the cIPK compared to the in vivo average in paper I (18.8).

In vivo, the clearance for albumin is underestimated due to tubular reabsorption and degradation of proteins that occur through uptake in the megalin/cubilin complex (27, 28, 55). The reabsorption of proteins from the primary urine has been demonstrated using micropuncture techniques both in vivo and in isolated perfused rats (161). Also, the uptake of filtered albumin along the nephron was illustrated using a fractional micropuncture technique by Tojo and Endou (165). The results in this thesis regarding albumin clearances are well in accordance with other studies in vivo (69, 161) and cIPK (69, 120, 121, 163). The reliability of the cIPK model is further emphasized by the clearance of the neutral inert Ficoll. The fractional clearance for Ficoll 35.5 Å, the neutral counterpart of albumin, was similar in all control groups and in accordance with observations in rats (69, 123, 124) and humans (9).

Low GFRs and filtration fractions in cIPK, compared to in vivo experiments, can be explained by the low temperature and the erythrocyte-free perfusate. At 37°C, the viscosity of the perfusate is $1/2 - 1/3$ of that in blood. In order to maintain a given arterial pressure the flow rate must be increased, thus reducing the filtration fraction by a factor of 2-3. However, low temperature (8°C) will increase the viscosity and thus partly compensate for the loss of erythrocytes. On the other hand, low temperature will reduce hydraulic conductivity by a factor of 2, according to Poiseuille's law, and increase tubular fluid viscosity. The increased tubular fluid

viscosity elevates the intratubular pressure causing a reduced GFR. The increased tubular fluid volume, caused by inhibited tubular reabsorption, raises tubular hydrostatic pressure further and reduces the filtration gradient across the glomerular capillary wall (79). Furthermore, there are fewer functionally active nephrons in the isolated perfused kidney with marked heterogeneity (97). All these effects reduce the magnitude of GFR and the absolute values of renal clearance, but the function of individual glomeruli and hence the fractional clearances are apparently not affected. Indeed, no difference has been found in fractional clearance for albumin between homogeneously and heterogeneously perfused kidneys (97). The unrestricted exchange area over diffusion distance is about one order of magnitude less in the cIPK than in vivo reflecting fewer active nephrons in the cIPK, but with unaltered glomerular permselectivity.

Mathematical models

In this thesis mainly two models of the glomerular barrier have been used: namely the heterogeneous charged fiber model (paper I) and the gel-membrane model (paper I-III). Both models were developed by us and describe size and charge selectivity of the glomerular barrier.

In the heterogeneous charged fiber model the surface charge of the fibers was set to -0.2 C/m^2 and a reduced fiber volume fraction could reflect a loss of charged fibers in the gel. However, theoretically there may also be a partial loss of surface charge of each fiber by the enzyme. It was decided to define the fiber charge as a constant and compare the fiber volume fraction of the charged fibers since separation of the two factors would require additional information using solutes of different molecular charge. In paper I, heterogeneity was introduced into the charged fiber model. Hereby, the adaptation to the experimentally determined Ficoll data improved dramatically (Figure 25).

The gel-membrane model estimates size selectivity with the two-pore model and charge selectivity through calculation of the charge density in the glomerular barrier. The estimated charge density of $\sim 50 \text{ mEq/L}$ in controls is similar to that previously estimated by us in the rat (69, 120, 121, 163). Two-pore model analysis in cIPK controls gave a functional small pore radius between $45.8\text{-}47.2 \text{ \AA}$, and between $96\text{-}167 \text{ \AA}$ for the less frequent large pore. The results concerning pore sizes are well in accordance with our previous studies in rats (69, 120, 121, 163). Nevertheless, both of these models represent oversimplifications of reality. For example, the charged fiber model assumes interaction between a solute and one fiber. In reality, the solute will interact with multiple fibers since the glomerular barrier is highly complex and contains plasma proteins as well (43, 130). The gel-membrane model, for the sake of simplicity, separates charge from size selectivity. Naturally, such a separation can not occur in real barriers. Also, both models describe the glomerular barrier as one homogeneous layer, but the glomerular barrier in fact consists of several different layers and cells, see Introduction. Still, as seen in figure 25, the fit between biological data and model estimated data is

excellent. We use both these models to partly correct for possible flaws in the theories. The results, however, are remarkably similar.

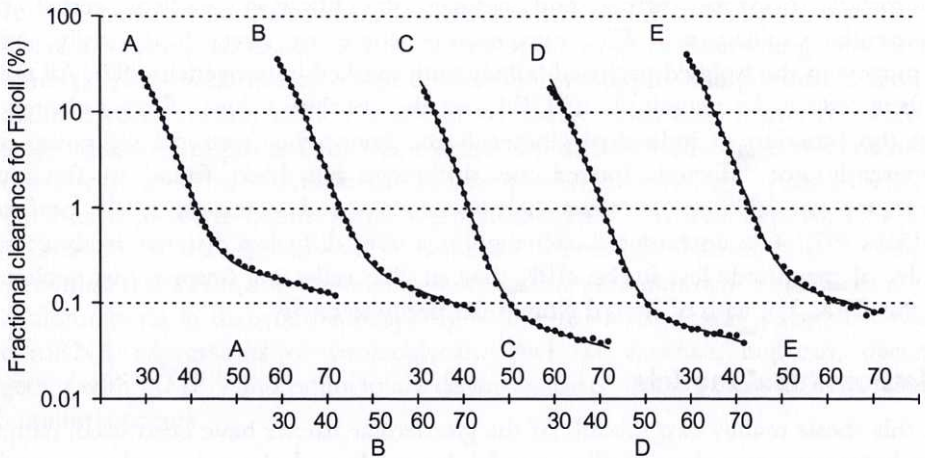


Figure 25. The fit between experimentally determined (●) and modeled (—) fractional clearances for Ficoll 30-70 Å in four representative control experiments using the heterogeneous charged fiber model. Each curve has a separate scale on the x-axis.

Endothelial cell glycocalyx and charge selectivity

The finding that the fractional clearance for the negatively charged albumin is much lower than that for Ficoll of equivalent size supports the classical notion of a charge barrier. As reviewed in the introduction, the concept of charge selectivity has been questioned by Comper and coworkers (125, 143). However, we have in numerous papers described the presence of glomerular charge selectivity (76, 96, 119, 121, 163). Also, in a recent paper by Deen and Lazzara (42) a model was developed to describe the variability of albumin concentrations in proximal tubular fluid. They concluded that the high albumin clearances proposed by Comper and coworkers (125, 143) are not compatible with the micropuncture data mentioned above.

In order to investigate the composition of the glomerular endothelial cell glycocalyx and the functional properties of the glomerular barrier when altering the glycocalyx, different GAG digesting enzymes were used. The morphological alteration of the glycocalyx after enzyme digestion was visualized indirectly with Intralipid[®] droplets and electron microscopy. Digestion of the glycocalyx with either enzyme, i.e. hyaluronidase, heparinase and chondroitinase, led to an increased relative frequency of Intralipid[®] droplets in the zone closest to the endothelium. The main interest was to compare controls to enzyme treated animals rather than measuring the actual thickness of the glycocalyx. Hence, dehydration following tissue fixation is not a problem in this study. The kidneys were flow-arrested which rules out a flow-dependent distribution of the Intralipid[®] droplets. Also, Bowman's capsule should protect glomerular capillaries from changed morphology due to an increased

intrarenal pressure when using subcapsular injections.

Functional aspects of glomerular filtration after enzyme digestion were studied in the cIPK at 8°C. The fractional clearance for albumin was increased up to 5-fold after treatment with hyaluronidase and the high dose of chondroitinase. The fractional clearance for Ficoll 35.5 Å, the neutral counterpart of albumin, was similar in all groups. Data from the heterogeneous charged fiber model in paper I and the gel-membrane model with the two-pore model in paper II showed that the size selectivity of the glomerular barrier was unaltered by all enzyme treatments. The same models revealed that hyaluronidase and the high doses of heparinase and chondroitinase resulted in a decreased fraction of negatively charge fibers (paper I) or a decreased charge density (paper II) in the glomerular barrier.

It can be argued that the enzymes may have damaged the barrier elsewhere than at the glycocalyx level. However, we found no ultrastructural changes of endothelial cells, GBM, or podocytes after enzyme treatment. Also, the morphological experiments in paper II support the notion of endothelial cell glycocalyx digestion. Moreover, the enzymes used are large molecules; molecular weights are approximately 56 kDa, 71 kDa and 120 kDa for hyaluronidase, heparinase, and chondroitinase, respectively. Thus, the enzyme concentration was highest intravascularly and the concentration gradient expected to be 2-3 orders of magnitude across the glomerular barrier.

In several papers (7, 30, 60, 67, 76, 120, 164) we have discussed the importance of the glomerular endothelial cell glycocalyx for charge selectivity. Placing the charge barrier at the endothelial cell glycocalyx could explain the reversible alteration in charge density when altering perfusate ionic strength (30, 164). It has also been shown that glomerular permeability is affected by plasma composition (61, 78), supporting the idea of an intimate relationship between charge selectivity and plasma, probably exerted by the endothelial cell glycocalyx.

The glomerular barrier in diabetes

In paper III, the hitherto most extensive analysis of glomerular size and charge selectivity in mice with long term diabetes is presented. The functional alterations behind albuminuria were further examined by observing the gene expression of components in the glomerular barrier.

The NOD-mouse is an established model of spontaneous insulin-dependent diabetes mellitus type I (IDDM) (32, 100), see Introduction. Morphological changes after 10 weeks of diabetes (45, 99) preceded the albuminuria that in our hands was indicated after 27 weeks in vivo. In humans, diabetic nephropathy is a late complication occurring progressively in susceptible patients after 25-30 years of diabetes (see Introduction), which probably corresponds to 25-30 weeks in mice with their shorter lifespan. Proteinuria in diabetes has been suggested to originate from alteration of either size (39, 53, 113, 166) or charge selectivity (6, 38, 39, 94, 128, 144) or both (2, 167). However, these studies were all done in vivo and the controversy may be due to methodological differences and limitations as discussed

above.

We found an increased fractional clearance for albumin after 40 weeks of diabetes without any change for Ficoll 35.5 Å, the neutral counterpart of albumin, indicating altered glomerular charge selectivity. Glomerular size and charge selectivity was estimated using the gel-membrane model. The charge density in the glomerular barrier was found to be decreased after 40 weeks of diabetes. The results regarding pore sizes and charge density in controls are well in accordance with our previous studies in rats (68, 120, 121, 163) and mice (76).

Gene regulation in diabetic nephropathy

The second object of paper III was to correlate the observed functional changes with molecular alterations. Thus, we investigated two podocyte specific proteins (nephrin and podocin) together with matrix metalloprotease-9, protein kinase C, and several proteoglycan core proteins (Table 2). The reason for our interest in proteoglycans is that they are likely to play a crucial role in the microvascular permeability in all organs including the kidney (76).

Versican

One of the most prominent changes induced by diabetes was the decreased expression of versican mRNA to less than half of that in controls. Versican is an extracellular matrix proteoglycan with chondroitin sulfate chains that is able to bind hyaluronic acid (74). We have recently found versican to be expressed by human glomerular endothelial cells (7) and all of the four versican isoforms can be found in the human kidney (V_0 - V_3) (22). In the umbilical vein, versican was found in significant levels on the endothelial surface whereas only the smooth muscle cells in arteries stained positive (172). Down-regulation of versican may cause altered glomerular endothelial cell glycocalyx composition and reduced charge selectivity. This could explain the functional changes observed in the diabetic animals at week 40 when glomerular charge selectivity was altered.

The nephrosis inducing agent puromycin aminonucleoside (PAN) decreased the expression of versican when applied to human glomerular endothelial cells in culture (7). Similar observations were made in rats with nephrotic syndrome induced with PAN (8). In contrast, versican is up-regulated by platelet derived growth factor (PDGF) in cultured arterial smooth muscle cells (48, 148, 149), and versican accumulation in smooth muscle is believed to play a key role in atherosclerosis and restenosis (176). Also, mesangial cells cultured under high glucose conditions increased their versican mRNA and protein expression (171, 175). However, data from non-mesangial cells in the glomerular barrier, cultured under hyperglycemic conditions, are incomplete. The role for versican seems to differ between different tissues and cell types, which may be due to different distribution of the isoforms and a different ratio of chondroitin 6-sulfate to chondroitin 4-sulfate.

Decorin

The finding of a down-regulation of the decorin core protein fits with the notion that this proteoglycan binds and neutralizes extracellular transforming growth factor β (TGF- β), thus antagonizing the pro-sclerotic effect of this cytokine (13, 14). Previous studies have reported an up-regulation of decorin mRNA in the early phase (1-6 weeks) of diabetes in mice (112) and in mesangial cells cultured under high glucose conditions (112, 171). Indeed, at week 10 we observed a tendency towards an up-regulation of decorin (Figure 23). Interestingly, administration of decorin inhibits TGF- β mediated extracellular matrix expression in experimental nephritis (13), suggesting an important role for decorin also in diabetic nephropathy.

MMP-9

Accumulation of extracellular matrix can result from either an increased synthesis or a decreased degradation. Normally, extracellular matrix is degraded primarily by matrix metalloproteases (MMP) (36). The activity of MMP is controlled at multiple steps, including their level of synthesis as inactive proenzymes, activation of the proenzymes by plasmin, and inhibition of the active enzyme by binding to tissue inhibitor of metalloprotease (TIMP). However, studies on mesangial cells cultured under high glucose conditions suggest that plasmin activity is reduced by the up-regulated expression of plasminogen activator inhibitor (PAI-1) (1, 50). In this study MMP-9 was found to be down-regulated in diabetes, thus probably contributing to increased glomerular basement membrane thickness and extracellular matrix expansion. Our data on MMP-9 confirm the observation in a recent report after 6 months of streptozotocin induced diabetes in rats (107). Also, mesangial cells cultured under high glucose conditions or with glycated albumin have a decreased expression of MMP-9 (106, 186).

Podocin

The gene expression of the podocyte-specific slit diaphragm protein podocin was markedly down-regulated after 40 weeks of diabetes. Podocin is a key protein in certain nephrotic syndromes (15). This is, however, the first report of altered gene expression of podocin in diabetic nephropathy. We also found a tendency of decreased expression of nephrin at week 10 and 40, and for podocin at week 10 (Figure 23). Other studies have shown that the expression of the podocyte specific protein nephrin is down-regulated in diabetic patients (89) and diabetic rats (82) with proteinuria. The decrease in expression of podocin could reflect a podocyte loss, but the number of cells does not seem to change during the course of diabetes (160). In addition, it has been described that treatment with the angiotensin converting enzyme inhibitor (ACEi) perindopril reversed the down-regulated nephrin expression in diabetes (82, 89), suggesting altered synthesis in the cells present in the glomerular barrier.

Therapies in diabetic nephropathy

Intracellular hyperglycemia alters the expression of several factors which in turn leads to a cascade of events (19). Key molecules are thought to be TGF- β , the formation of advanced glycated end-products (AGE), and reactive oxygen species (ROS)(19, 101). Numerous studies indicate that hyperglycemia induces an increase in TGF- β expression of mRNA and protein in experimental and human diabetes (75, 127, 153-155, 174, 184) as well as in cultured mesangial cells (84, 85, 171). Moreover, in experimental models of diabetes glomerular injury was prevented by intervention directed against ROS and AGE (31, 33, 52, 116, 158, 169).

In patients, the progression of diabetic nephropathy can be slowed down with angiotensin converting enzyme inhibitors (ACEi) and angiotensin receptor blockers (ARB) separately or in combination (58, 62, 90, 162). The beneficial effects of ACEi and ARB can only partly be attributed to effective control of systemic and intraglomerular hypertension; hence there seem to be other renoprotective effects as well. The beneficial effects on renal function by ACEi have been shown for other nephropathies as well (129, 132, 141). Interestingly, the ARB captopril decreased the plasma levels of TGF- β in hypertensive kidney transplant patients (46).

Furthermore, as reviewed by Gambaro and Woude (54), heparin and GAG have been shown to reduce the albumin excretion rate in diabetic patients with albuminuria. The authors suggest this to be related to the effect of heparin on extracellular matrix and protein synthesis, rather than correcting the charge deficiency by adhering to the glomerular barrier. In addition, as mentioned above, administration of decorin inhibits TGF- β mediated extracellular matrix expression in experimental nephritis (13).

CONCLUDING REMARKS

The general aim of this thesis was to evaluate macromolecular transport over the glomerular barrier under physiological and pathophysiological conditions. To accomplish this, a new mouse model was developed for studying the glomerular barrier, the cooled isolated perfused kidney at 8°C.

This thesis demonstrates that the glomerular barrier indeed is highly charge selective, in correspondence with the classical view. This is reflected by the much lower fractional clearance for albumin compared to the neutral counterpart Ficoll 35.5 Å. Also, the importance for GAGs in maintaining charge selectivity is described. Thus, digestion with GAG degrading enzymes increased the fractional clearance for albumin up to 5-fold without affecting the neutral Ficoll 35.5 Å. In this thesis, the first evidence that morphological alterations in endothelial cell glycocalyx have functional consequences for glomerular permeability is presented. This suggest that the endothelial cell glycocalyx have charge selective properties.

Albuminuria in diabetic nephropathy originates from an alteration in charge selectivity. This thesis provides the first description of an alteration in gene expression of versican, a glycocalyx component, and podocin, a slit diaphragm component, in long term diabetes. The reduced expression of MMP-9 reflects the diminished turn-over of some proteoglycans and collagen IV. These findings support the idea that diabetic nephropathy may be treated by interfering with proteoglycan synthesis and degradation.

FUTURE PERSPECTIVES

To further examine the role of GAGs in glomerular charge selectivity, genetic models of altered GAG composition will be of importance. GAGs are important during development and genetic modifications of GAG metabolism sometimes leads to embryonal or juvenile death. For this reason animals, in which the genetic modification is inducible and/or tissue-specific, will be needed. There are also methods for isolation of the luminal side of the plasma membrane and its proteins on the endothelial cells, proteins which would be of great interest to investigate further. Hyaluronic acid has no protein core which makes it more difficult to study than other GAGs, however, we have demonstrated a role for hyaluronic acid in the glycocalyx and will further investigate this.

This thesis present some interesting data in long term diabetes and the same model would be useful to study the effects of established drugs such as ACEi and ARB and more experimental ones like decorin. Also, studies on cultured glomerular endothelial cells with addition of TGF- β or glucose are of high interest since the literature is incomplete and the mesangial cells are by far the most studied.

It would also be interesting to further investigate mRNA and protein expression in different models of nephrotic syndromes, both experimental models and patients. Biopsies from nephrotic patents are studied in an ongoing project in our laboratory.

SVENSK SAMMANFATTNING

Varje dag filtreras 180 liter plasma över kapillärväggarna i njurens glomeruli. Denna glomerulära barriär har under normala förhållanden extremt låg genomsläpplighet för makromolekyler, t.ex. negativt laddat albumin, samtidigt som vatten och små molekyler i stort sett filtreras fritt. När molekyler som albumin läcker igenom barriären till urinen tyder detta på njursjukdom. Den glomerulära barriären har storleks- och laddningsselektiva egenskaper och består av tre skikt; glomerulära fenestrerade endotelceller med ett negativt laddat gel-täcke eller glykokalyx, det glomerulära basalmembranet samt podocyter.

I den här avhandlingen har det undersökts om glykokalyx på endotelcellerna kan vara viktig för barriärens laddningsselektiva egenskaper. Studierna är baserade på funktion, morfologi och molekylärt uttryck i friska, glykokalyxmodifierade och diabetiska njurar. För att studera funktionen av den glomerulära barriären utan modifiering av primärurinen perfunderades njurarna vid 8°C.

I njurar där glykokalyx togs bort med enzymer riktade mot glukos/galaktosaminoglykaner ökade albuminläckaget upp till 5 gånger jämfört med kontroller. Detta beror på en skada i njurens laddningsbarriär eftersom filtrationen av den neutrala motsvarigheten till albumin, Ficoll 35.5 Å, var oförändrad. Enzyminducerade förändringar av glykokalyx studerades också morfologiskt i elektronmikroskop, där tjockleken på glykokalyx indirekt visades med Intralipid® droppar.

Möss som spontant utvecklar diabetes typ I studerades för att klargöra om ökat läckage av albumin vid diabetes beror på skador i storleks- eller laddningsbarriären. Mössen studerades i 10 eller 40 veckor. Efter 40 veckor med diabetes visade sig albuminläckaget ha ökat 3 gånger jämfört med kontroll. Även här visar det sig bero på en skada i njurens laddningsbarriär eftersom filtrationen av den neutrala motsvarigheten till albumin, Ficoll 35.5 Å, var oförändrad. Realtids-PCR avslöjade en rad nedregleringar av mRNA i njuren efter 40 veckor med diabetes. Proteoglykanerna versican, decorin och biglycan var nedreglerade tillsammans med podocin och matrixmetalloproteas-9.

Denna avhandling beskriver vikten av ett intakt endotelcellsglykokalyx för att behålla njurens laddnings selektivitet. Avhandlingen visar också att albuminläckaget vid diabetesnefropati beror på minskad laddningsselektivitet. Albuminuri vid diabetes är kopplat till nedreglering av flera gener, däribland versican som finns i endotelcellernas glykokalyx.

ACKNOWLEDGEMENTS

I wish to express my sincere gratitude to all who have contributed to this work, and especially to:

Professor **Börje Haraldsson**, my supervisor, thanks for never-ending support, enthusiasm, encouragement, and for being such an excellent tutor.

Anna Björnson Granqvist, coauthor, for nice collaboration, friendship, fun times, and support in the ups and downs of science.

Jenny Nyström, coauthor, for pleasant collaboration, friendship and much appreciated discussions.

Ulf Nilsson for support, interesting discussions, and all the proofreading.

Clara Hjalmarsson, Kerstin Olsson, and Maria Ohlson for nice collaboration and fun times.

Professor **Bengt Johansson** for interesting discussions and for teaching me all I know about electron microscopy.

Emelie Roos for always helping out with animals and HPLC.

Yvonne Josefsson and **Gunnel Bokhede** for preparing endless specimens.

Elisabeth Ericsson, Lisbeth Selven, and Inga-Britt Persson for always being kind and helpful.

Past and present friends and colleagues at the Renal Center: **Bergur, Elisabeth, Inger, Yun, Daina, Peter, Gregor, Nicoletta, and Martina.**

Professor **Thomas Jansson**, professor **Ove Lundgren**, and **Mats Jodal** for creating an inspiring scientific atmosphere at the department.

Anna-Lena Dahlgren and **Kerstin Hörnberg** for excellent secretarial services.

Arne Larsson for help with library matters and **Lars Stage** for invaluable help with the lab-equipment.

All other friends and colleagues at the Department of Physiology and especially to all PhD students for fun discussions and parties.

Family and friends for love and support!

This study was supported by the Swedish Medical Research Council, the Knut and Alice Wallenberg Research Foundation, the IngaBritt and Arne Lundberg Foundation, the National Association of Kidney Disease, the Willhem and Martin Lundgren Foundation, the John and Brit Wennerströms Foundation, and the Sahlgrenska University Hospital Grant LUA-7545

REFERENCES

1. **Abdel Wahab N and Mason RM.** Modulation of neutral protease expression in human mesangial cells by hyperglycaemic culture. *Biochem J* 320 (Pt 3): 777-783, 1996.
2. **Andersen S, Blouch K, Bialek J, Deckert M, Parving HH, and Myers BD.** Glomerular permselectivity in early stages of overt diabetic nephropathy. 58: 2129, 2000.
3. **Andersson RN.** Deaths: leading causes for 2000. *National Vital Stat Report* 50: 1-85, 2002.
4. **Atkinson MA and Leiter EH.** The NOD mouse model of type 1 diabetes: as good as it gets? *Nat Med* 5: 601-604, 1999.
5. **Avasthi PS and Koshy V.** Pathophysiology and clinical relevance of proteinuria: glomerular endothelial glycocalyx. 68: 104, 1988.
6. **Bangstad HJ, Kofoed-Enevoldsen A, Dahl-Jorgensen K, and Hanssen KF.** Glomerular charge selectivity and the influence of improved blood glucose control in type 1 (insulin-dependent) diabetic patients with microalbuminuria. *Diabetologia* 35: 1165-1169, 1992.
7. **Bjornson A, Moses J, Ingemansson A, Haraldsson B, and Sorensson J.** Primary human glomerular endothelial cells produce proteoglycans and puromycin affects their posttranslational modification. *Am J Physiol Renal Physiol*, 2004.
8. **Björnson Granqvist A.** Functional and molecular aspects of the glomerular barrier. *Ph D Thesis*, 2004.
9. **Blouch K, Deen WM, Fauvel JP, Bialek J, Derby G, and Myers BD.** Molecular configuration and glomerular size selectivity in healthy and nephrotic humans. *Am J Physiol Renal Physiol* 273: F430, 1997.
10. **Bojestig M, Arnqvist HJ, Hermansson G, Karlberg BE, and Ludvigsson J.** Declining incidence of nephropathy in insulin-dependent diabetes mellitus. *N Engl J Med* 330: 15-18, 1994.
11. **Bojestig M, Arnqvist HJ, Karlberg BE, and Ludvigsson J.** Glycemic control and prognosis in type 1 diabetic patients with microalbuminuria. *Diabetes Care* 19: 313-317, 1996.
12. **Bolton GR, Deen WM, and Daniels BS.** Assessment of the charge selectivity of glomerular basement membrane using Ficoll sulfate. 274: F889, 1998.
13. **Border WA, Noble NA, Yamamoto T, Harper JR, Yamaguchi Y, Pierschbacher MD, and Ruoslahti E.** Natural inhibitor of transforming growth factor-beta protects against scarring in experimental kidney disease. *Nature* 360: 361-364, 1992.
14. **Border WA, Noble NA, Yamamoto T, Tomooka S, and Kagami S.** Antagonists of transforming growth factor-beta: a novel approach to treatment of glomerulonephritis and prevention of glomerulosclerosis. *Kidney Int* 41: 566-570, 1992.

15. **Boute N, Gribouval O, Roselli S, Benessy F, Lee H, Fuchshuber A, Dahan K, Gubler MC, Niaudet P, and Antignac C.** NPHS2, encoding the glomerular protein podocin, is mutated in autosomal recessive steroid-resistant nephrotic syndrome. *Nat Genet* 24: 349-354, 2000.
16. **Bray J and Robinson GB.** Influence of charge on filtration across renal basement membrane films in vitro. 25: 527, 1984.
17. **Brenner BM, Hostetter TH, and Humes HD.** Glomerular permselectivity: barrier function based on discrimination of molecular size and charge. *Am J Physiol* 234: F455-460, 1978.
18. **Breyer MD, Bottinger E, Brosius FC, 3rd, Coffman TM, Harris RC, Heilig CW, and Sharma K.** Mouse Models of Diabetic Nephropathy. *J Am Soc Nephrol* 16: 27-45, 2005.
19. **Brownlee M.** Biochemistry and molecular cell biology of diabetic complications. 414: 813, 2001.
20. **Cameron MJ, Meagher C, and Delovitch TL.** Failure in immune regulation begets IDDM in NOD mice. *Diabetes Metab Rev* 14: 177-185, 1998.
21. **Caramori ML, Fioretto P, and Mauer M.** The need for early predictors of diabetic nephropathy risk: is albumin excretion rate sufficient? *Diabetes* 49: 1399-1408, 2000.
22. **Cattaruzza S, Schiappacassi M, Ljungberg-Rose A, Spessotto P, Perissinotto D, Morgelin M, Mucignat MT, Colombatti A, and Perris R.** Distribution of PG-M/versican variants in human tissues and de novo expression of isoform V3 upon endothelial cell activation, migration, and neoangiogenesis in vitro. *J Biol Chem* 277: 47626-47635, 2002.
23. **Caulfield JP and Farquhar MG.** Distribution of anionic sites in glomerular basement membranes: their possible role in filtration and attachment. 73: 1646, 1976.
24. **Chang RL, Deen WM, Robertson CR, and Brenner BM.** Permselectivity of the glomerular capillary wall: III. Restricted transport of polyanions. 8: 212, 1975.
25. **Charnock JS, Doty DM, and Russel JC.** The effect of temperature on the activity of Na⁺/K⁺-ATPase. 142: 633, 1971.
26. **Chavers BM, Bilous RW, Ellis EN, Steffes MW, and Mauer SM.** Glomerular lesions and urinary albumin excretion in type I diabetes without overt proteinuria. *N Engl J Med* 320: 966-970, 1989.
27. **Christensen EI and Birn H.** Megalin and cubilin: synergistic endocytic receptors in renal proximal tubule. 280: F562, 2001.
28. **Christensen EI and Verroust PJ.** Megalin and cubilin, role in proximal tubule function and during development. *Pediatr Nephrol* 17: 993-999, 2002.
29. **Chua SC, Jr., Chung WK, Wu-Peng XS, Zhang Y, Liu SM, Tartaglia L, and Leibel RL.** Phenotypes of mouse diabetes and rat fatty due to mutations in the OB (leptin) receptor. *Science* 271: 994-996, 1996.

30. **Ciarimboli G, Hjalmarsson C, Bokenkamp A, Schurek HJ, and Haraldsson B.** Dynamic alterations of glomerular charge density in fixed rat kidneys suggest involvement of endothelial cell coat. 285: F722, 2003.
31. **Cohen MP, Masson N, Hud E, Ziyadeh F, Han DC, and Clements RS.** Inhibiting albumin glycation ameliorates diabetic nephropathy in the db/db mouse. *Exp Nephrol* 8: 135-143, 2000.
32. **Craighead JE.** Experimental models of juvenile onset (insulin-dependent) diabetes mellitus. *Monogr Pathol* 21: 166-176, 1980.
33. **Craven PA, Melhem MF, Phillips SL, and DeRubertis FR.** Overexpression of Cu²⁺/Zn²⁺ superoxide dismutase protects against early diabetic glomerular injury in transgenic mice. *Diabetes* 50: 2114-2125, 2001.
34. **Daniels BS.** Increased albumin permeability in vitro following alterations of glomerular charge is mediated by the cells of the filtration barrier. 124: 224, 1994.
35. **David G.** Integral membrane heparan sulfate proteoglycans. *Faseb J* 7: 1023-1030, 1993.
36. **Davies M, Coles GA, Thomas GJ, Martin J, and Lovett DH.** Proteinases and the glomerulus: their role in glomerular diseases. *Klin Wochenschr* 68: 1145-1149, 1990.
37. **Deckert T, Feldt-Rasmussen B, Borch-Johnsen K, Jensen T, and Kofoed-Enevoldsen A.** Albuminuria reflects widespread vascular damage. The Steno hypothesis. *Diabetologia* 32: 219-226, 1989.
38. **Deckert T, Feldt-Rasmussen B, Djurup R, and Deckert M.** Glomerular size and charge selectivity in insulin-dependent diabetes mellitus. *Kidney Int* 33: 100-106, 1988.
39. **Deckert T, Kofoed-Enevoldsen A, Vidal P, Norgaard K, Andreassen HB, and Feldt-Rasmussen B.** Size- and charge selectivity of glomerular filtration in Type 1 (insulin-dependent) diabetic patients with and without albuminuria. *Diabetologia* 36: 244-251, 1993.
40. **Deen WM.** What determines glomerular capillary permeability? *J Clin Invest* 114: 1412-1414, 2004.
41. **Deen WM, Bridges CR, Brenner BM, and Myers BD.** Heteroporous model of glomerular size selectivity: application to normal and nephrotic humans. *Am J Physiol* 249: F374, 1985.
42. **Deen WM and Lazzara MJ.** Glomerular filtration of albumin: how small is the sieving coefficient? *Kidney Int Suppl*: S63-64, 2004.
43. **Deen WM, Lazzara MJ, and Myers BD.** Structural determinants of glomerular permeability. *Am J Physiol Renal Physiol* 281: F579, 2001.
44. **DeFronzo RA and Reasner C.** The Diabetes Control and Complications Trial Study: implications for the diabetic foot. *J Foot Ankle Surg* 33: 551-556, 1994.

45. **Doi T, Hattori M, Agodoa LY, Sato T, Yoshida H, Striker LJ, and Striker GE.** Glomerular lesions in nonobese diabetic mouse: before and after the onset of hyperglycemia. *63: 204, 1990.*
46. **el-Agroudy AE, Hassan NA, Foda MA, Ismail AM, el-Sawy EA, Mousa O, and Ghoneim MA.** Effect of angiotensin II receptor blocker on plasma levels of TGF-beta 1 and interstitial fibrosis in hypertensive kidney transplant patients. *Am J Nephrol 23: 300-306, 2003.*
47. **Esmann M and Skou JC.** Temperature-dependencies of various catalytic activities of membrane-bound Na⁺/K⁺-ATPase from ox brain, ox kidney and shark rectal gland and of C12E8-solubilized shark Na⁺/K⁺-ATPase. *944: 344, 1988.*
48. **Evanko SP, Johnson PY, Braun KR, Underhill CB, Dudhia J, and Wight TN.** Platelet-derived growth factor stimulates the formation of versican-hyaluronan aggregates and pericellular matrix expansion in arterial smooth muscle cells. *Arch Biochem Biophys 394: 29-38, 2001.*
49. **Fagot-Campagna A, Pettitt DJ, Engelgau MM, Burrows NR, Geiss LS, Valdez R, Beckles GL, Saaddine J, Gregg EW, Williamson DF, and Narayan KM.** Type 2 diabetes among North American children and adolescents: an epidemiologic review and a public health perspective. *J Pediatr 136: 664-672, 2000.*
50. **Fisher EJ, McLennan SV, Yue DK, and Turtle JR.** High glucose reduces generation of plasmin activity by mesangial cells. *Microvasc Res 53: 173-178, 1997.*
51. **Fogh-Andersen N, Bjerrum PJ, and Siggaard-Andersen O.** Ionic binding, net charge, and Donnan effect of human serum albumin as a function of pH. *Clin Chem 39: 48-52, 1993.*
52. **Forbes JM, Soulis T, Thallas V, Panagiotopoulos S, Long DM, Vasan S, Wagle D, Jerums G, and Cooper ME.** Renoprotective effects of a novel inhibitor of advanced glycation. *Diabetologia 44: 108-114, 2001.*
53. **Friedman S, Jones HW, 3rd, Golbetz HV, Lee JA, Little HL, and Myers BD.** Mechanisms of proteinuria in diabetic nephropathy. II. A study of the size-selective glomerular filtration barrier. *Diabetes 32 Suppl 2: 40-46, 1983.*
54. **Gambaro G and van der Woude FJ.** Glycosaminoglycans: use in treatment of diabetic nephropathy. *J Am Soc Nephrol 11: 359-368, 2000.*
55. **Gekle M.** Renal tubule albumin transport. *Annu Rev Physiol 67: 573-594, 2005.*
56. **Goode NP, Shires M, Crellin MD, and Davison AM.** Detection of glomerular anionic sites in post-embedded ultra-thin sections using cationic colloidal gold. *39: 965, 1991.*
57. **Groffen AJ, Veerkamp JH, Monnens LA, and van den Heuvel LP.** Recent insights into the structure and functions of heparan sulfate proteoglycans in the human glomerular basement membrane. *Nephrol Dial Transplant 14: 2119-2129, 1999.*
58. **Gross JL, de Azevedo MJ, Silveiro SP, Canani LH, Caramori ML, and Zelmanovitz T.** Diabetic nephropathy: diagnosis, prevention, and treatment. *Diabetes Care 28: 164-176, 2005.*

59. **Gu K, Cowie CC, and Harris MI.** Mortality in adults with and without diabetes in a national cohort of the U.S. population, 1971-1993. *Diabetes Care* 21: 1138-1145, 1998.
60. **Haraldsson B and Sorensson J.** Why do we not all have proteinuria? An update of our current understanding of the glomerular barrier. 19: 7, 2004.
61. **Haraldsson BS, Johnsson EK, and Rippe B.** Glomerular permselectivity is dependent on adequate serum concentrations of orosomucoid. 41: 310, 1992.
62. **Harris DC and Rangan GK.** Retardation of kidney failure -- applying principles to practice. *Ann Acad Med Singapore* 34: 16-23, 2005.
63. **Hasslacher C, Ritz E, Wahl P, and Michael C.** Similar risks of nephropathy in patients with type I or type II diabetes mellitus. *Nephrol Dial Transplant* 4: 859-863, 1989.
64. **He CJ, Zheng F, Stitt A, Striker L, Hattori M, and Vlassara H.** Differential expression of renal AGE-receptor genes in NOD mice: possible role in nonobese diabetic renal disease. 58: 1931, 2000.
65. **Henry CBS and Duling BR.** Permeation of the luminal capillary glycocalyx is determined by hyaluronan. 277: H508, 1999.
66. **Hildebrand A, Romaris M, Rasmussen LM, Heinegard D, Twardzik DR, Border WA, and Ruoslahti E.** Interaction of the small interstitial proteoglycans biglycan, decorin and fibromodulin with transforming growth factor beta. *Biochem J* 302 (Pt 2): 527-534, 1994.
67. **Hjalmarsson C, Johansson BR, and Haraldsson B.** Electron microscopic evaluation of the endothelial surface layer of glomerular capillaries. 67: 9, 2004.
68. **Hjalmarsson C, Ohlson M, and Haraldsson B.** Puromycin aminonucleoside damages the glomerular size barrier with minimal effects on charge density. *Am J Physiol Renal Physiol* 281: F503, 2001.
69. **Hjalmarsson C, Ohlson M, and Haraldsson B.** Puromycin aminonucleoside damages the glomerular size barrier with minimal effects on charge density. 281: F503, 2001.
70. **Honjo K, Doi K, Doi C, and Mitsuoka T.** Histopathology of streptozotocin-induced diabetic DBA/2N and CD-1 mice. *Lab Anim* 20: 298-303, 1986.
71. **Hostetter TH.** Diabetic Nephropathy. In: *The Kidney*, edited by Brenner BM and Rector FC: W.B. Saunders Company, p. 1695-1727, 1991.
72. **Hu FB, Stampfer MJ, Solomon CG, Liu S, Willett WC, Speizer FE, Nathan DM, and Manson JE.** The impact of diabetes mellitus on mortality from all causes and coronary heart disease in women: 20 years of follow-up. *Arch Intern Med* 161: 1717-1723, 2001.
73. **Iozzo RV.** The family of the small leucine-rich proteoglycans: key regulators of matrix assembly and cellular growth. *Crit Rev Biochem Mol Biol* 32: 141-174, 1997.
74. **Iozzo RV.** Matrix proteoglycans: from molecular design to cellular function. *Annu Rev Biochem* 67: 609-652, 1998.

75. **Iwano M, Kubo A, Nishino T, Sato H, Nishioka H, Akai Y, Kurioka H, Fujii Y, Kanauchi M, Shiiki H, and Dohi K.** Quantification of glomerular TGF-beta 1 mRNA in patients with diabetes mellitus. *Kidney Int* 49: 1120-1126, 1996.
76. **Jeansson M and Haraldsson B.** Glomerular size and charge selectivity in the mouse after exposure to glucosaminoglycan-degrading enzymes. 14: 1756, 2003.
77. **Johnson EJ and Deen WM.** Electrostatic effects on the equilibrium partitioning of spherical colloids in random fibrous media. *J Colloid Interface Sci* 178: 749, 1996.
78. **Johnsson E and Haraldsson B.** Addition of purified orosomucoid preserves the glomerular permeability for albumin in isolated perfused rat kidneys. *Acta Physiol Scand* 147: 1-8, 1993.
79. **Johnsson E, Rippe B, and Haraldsson B.** Analysis of the pressure-flow characteristics of isolated perfused rat kidneys with inhibited tubular reabsorption. 150: 189, 1994.
80. **Kanwar YS and Farquhar MG.** Anionic sites in the glomerular basement membrane. In vivo and in vitro localization to the laminae rarae by cationic probes. 81: 137, 1979.
81. **Kanwar YS and Farquhar MG.** Presence of heparan sulfate in the glomerular basement membrane. 76: 1303, 1979.
82. **Kelly DJ, Aaltonen P, Cox AJ, Rumble JR, Langham R, Panagiotopoulos S, Jerums G, Holthofer H, and Gilbert RE.** Expression of the slit-diaphragm protein, nephrin, in experimental diabetic nephropathy: differing effects of anti-proteinuric therapies. *Nephrol Dial Transplant* 17: 1327-1332, 2002.
83. **Kestila M, Lenkkeri U, Mannikko M, Lamerdin J, McCready P, Putaala H, Ruotsalainen V, Morita T, Nissinen M, Herva R, Kashtan CE, Peltonen L, Holmberg C, Olsen A, and Tryggvason K.** Positionally cloned gene for a novel glomerular protein--nephrin--is mutated in congenital nephrotic syndrome. *Mol Cell* 1: 575-582, 1998.
84. **Kolm-Litty V, Sauer U, Nerlich A, Lehmann R, and Schleicher ED.** High glucose-induced transforming growth factor beta1 production is mediated by the hexosamine pathway in porcine glomerular mesangial cells. *J Clin Invest* 101: 160-169, 1998.
85. **Kolm V, Sauer U, Olgemoeller B, and Schleicher ED.** High glucose-induced TGF-beta 1 regulates mesangial production of heparan sulfate proteoglycan. *Am J Physiol* 270: F812-821, 1996.
86. **Krege JH, Hodgin JB, Hagaman JR, and Smithies O.** A noninvasive computerized tail-cuff system for measuring blood pressure in mice. *Hypertension* 25: 1111-1115, 1995.
87. **Krege JH, John SW, Langenbach LL, Hodgin JB, Hagaman JR, Bachman ES, Jennette JC, O'Brien DA, and Smithies O.** Male-female differences in fertility and blood pressure in ACE-deficient mice. *Nature* 375: 146-148, 1995.
88. **Landau D, Segev Y, Afargan M, Silbergeld A, Katchko L, Podshyvalov A, and Phillip M.** A novel somatostatin analogue prevents early renal complications in the nonobese diabetic mouse. 60: 505, 2001.

89. **Langham RG, Kelly DJ, Cox AJ, Thomson NM, Holthofer H, Zaoui P, Pinel N, Cordonnier DJ, and Gilbert RE.** Proteinuria and the expression of the podocyte slit diaphragm protein, nephrin, in diabetic nephropathy: effects of angiotensin converting enzyme inhibition. *Diabetologia* 45: 1572-1576, 2002.
90. **Lee GS.** Retarding the progression of diabetic nephropathy in type 2 diabetes mellitus: focus on hypertension and proteinuria. *Ann Acad Med Singapore* 34: 24-30, 2005.
91. **Leiter EH.** Differential susceptibility of BALB/c sublines to diabetes induction by multi-dose streptozotocin treatment. *Curr Top Microbiol Immunol* 122: 78-85, 1985.
92. **Leiter EH.** Multiple low-dose streptozotocin-induced hyperglycemia and insulinitis in C57BL mice: influence of inbred background, sex, and thymus. *Proc Natl Acad Sci U S A* 79: 630-634, 1982.
93. **Leiter EH, Prochazka M, and Coleman DL.** The non-obese diabetic (NOD) mouse. *Am J Pathol* 128: 380-383, 1987.
94. **Lemley KV, Blouch K, Abdullah I, Boothroyd DB, Bennett PH, Myers BD, and Nelson RG.** Glomerular permselectivity at the onset of nephropathy in type 2 diabetes mellitus. *J Am Soc Nephrol* 11: 2095-2105, 2000.
95. **Lesley J, Hyman R, and Kincade PW.** CD44 and its interaction with extracellular matrix. *Adv Immunol* 54: 271-335, 1993.
96. **Lindstrom KE, Johnsson E, and Haraldsson B.** Glomerular charge selectivity for proteins larger than serum albumin as revealed by lactate dehydrogenase isoforms. *Acta Physiol Scand* 162: 481-488, 1998.
97. **Lindström K, Rönstedt L, Jaremko G, and Haraldsson B.** Physiological and morphological effects of perfusing isolated rat kidneys with hyperosmolar mannitol solutions. 166: 231, 1999.
98. **Ludwig DS and Ebbeling CB.** Type 2 diabetes mellitus in children: primary care and public health considerations. *Jama* 286: 1427-1430, 2001.
99. **Maeda M, Yabuki A, Suzuki S, Matsumoto M, Taniguchi K, and Nishinakagawa H.** Renal lesions in spontaneous insulin-dependent diabetes mellitus in the nonobese diabetic mouse: acute phase of diabetes. 40: 187, 2003.
100. **Makino S, Kunitomo K, Muraoka Y, Mizushima Y, Katagiri K, and Tochino Y.** Breeding of a non-obese, diabetic strain of mice. *Jikken Dobutsu* 29: 1-13, 1980.
101. **Mason RM and Wahab NA.** Extracellular matrix metabolism in diabetic nephropathy. *J Am Soc Nephrol* 14: 1358-1373, 2003.
102. **Mathews CE, Langley SH, and Leiter EH.** New mouse model to study islet transplantation in insulin-dependent diabetes mellitus. *Transplantation* 73: 1333-1336, 2002.
103. **Mauer SM, Lane P, Zhu D, Fioretto P, and Steffes MW.** Renal structure and function in insulin-dependent diabetes mellitus in man. *J Hypertens Suppl* 10: S17-20, 1992.

104. **Mauer SM, Steffes MW, Ellis EN, Sutherland DE, Brown DM, and Goetz FC.** Structural-functional relationships in diabetic nephropathy. *J Clin Invest* 74: 1143-1155, 1984.
105. **McCourt PA, Ek B, Forsberg N, and Gustafson S.** Intercellular adhesion molecule-1 is a cell surface receptor for hyaluronan. *J Biol Chem* 269: 30081-30084, 1994.
106. **McLennan SV, Fisher E, Martell SY, Death AK, Williams PF, Lyons JG, and Yue DK.** Effects of glucose on matrix metalloproteinase and plasmin activities in mesangial cells: possible role in diabetic nephropathy. *Kidney Int Suppl* 77: S81-87, 2000.
107. **McLennan SV, Kelly DJ, Cox AJ, Cao Z, Lyons JG, Yue DK, and Gilbert RE.** Decreased matrix degradation in diabetic nephropathy: effects of ACE inhibition on the expression and activities of matrix metalloproteinases. *Diabetologia* 45: 268-275, 2002.
108. **Mogensen CE.** The effect of blood pressure intervention on renal function in insulin-dependent diabetes. *Diabete Metab* 15: 343-351, 1989.
109. **Mogensen CE.** Long-term antihypertensive treatment inhibiting progression of diabetic nephropathy. *Br Med J (Clin Res Ed)* 285: 685-688, 1982.
110. **Mogensen CE.** Microalbuminuria and hypertension with focus on type 1 and type 2 diabetes. *J Intern Med* 254: 45-66, 2003.
111. **Mogensen CE and Schmitz O.** The diabetic kidney: from hyperfiltration and microalbuminuria to end-stage renal failure. *Med Clin North Am* 72: 1465-1492, 1988.
112. **Mogyorosi A and Ziyadeh FN.** Increased decorin mRNA in diabetic mouse kidney and in mesangial and tubular cells cultured in high glucose. *Am J Physiol* 275: F827-832, 1998.
113. **Nakamura Y and Myers BD.** Charge selectivity of proteinuria in diabetic glomerulopathy. *Diabetes* 37: 1202-1211, 1988.
114. **National Institute of Diabetes and Digestive and Kidney Diseases. Bethesda M.** National Diabetes Statistics fact sheet: general information and national estimates on diabetes in the United States, 2003. Rev. ed. 2004. U.S. Department of health and Human Services, National Institute of Health. <http://diabetes.niddk.nih.gov>, Publication No. 05-3892, 2004.
115. **National Institute of Diabetes and Digestive and Kidney Diseases. National Kidney and Urologic Diseases Information Clearinghouse. Bethesda M.** U.S. Department of health and Human Services, National Institute of Health. <http://diabetes.niddk.nih.gov>, NIH Publication No. 04-3925, 2003.
116. **Nicholls K and Mandel TE.** Advanced glycosylation end-products in experimental murine diabetic nephropathy: effect of islet isografting and of aminoguanidine. *Lab Invest* 60: 486-491, 1989.
117. **Ninomiya H, Inomata T, and Ogihara K.** Glomerular vascular changes in KK-Ay mice with early diabetes: scanning electron microscopy of vascular resin casts. *J Vet Med Sci* 60: 103-106, 1998.

118. **Ogston AG.** The spaces in a uniform random suspension of fibres. *Trans Faraday Soc* 54: 1754, 1958.
119. **Ohlson M, Sorensson J, Lindstrom K, Blom AM, Fries E, and Haraldsson B.** Effects of filtration rate on the glomerular barrier and clearance of four differently shaped molecules. *Am J Physiol Renal Physiol* 281: F103-113, 2001.
120. **Ohlson M, Sörensson J, and Haraldsson B.** A gel-membrane model of glomerular charge and size selectivity in series. 280: F396, 2001.
121. **Ohlson M, Sörensson J, and Haraldsson B.** Glomerular size and charge selectivity in the rat as revealed by FITC-Ficoll and albumin. 279: F84, 2000.
122. **Okazaki M, Saito Y, Udaka Y, Maruyama M, Murakami H, Ota S, Kikuchi T, and Oguchi K.** Diabetic nephropathy in KK and KK-Ay mice. *Exp Anim* 51: 191-196, 2002.
123. **Oliver JD, Anderson S, Troy JL, Brenner BM, and Deen WH.** Determination of glomerular size-selectivity in the normal rat with Ficoll. 3: 214, 1992.
124. **Oliver JD, Simons JL, Troy JL, Provoost AP, Brenner BM, and Deen WM.** Proteinuria and impaired glomerular permselectivity in uninephrectomized fawn-hooded rats. *Am J Physiol* 267: F917, 1994.
125. **Osicka TM, Pratt LM, and Comper WD.** Glomerular capillary wall permeability to albumin and horseradish peroxidase. 2: 199, 1996.
126. **Osterloh K, Ewert U, and Pries AR.** Interaction of albumin with the endothelial cell surface. *Am J Physiol Heart Circ Physiol* 283: H398-405, 2002.
127. **Park IS, Kiyomoto H, Abboud SL, and Abboud HE.** Expression of transforming growth factor-beta and type IV collagen in early streptozotocin-induced diabetes. *Diabetes* 46: 473-480, 1997.
128. **Pietravalle P, Morano S, Cristina G, De Rossi MG, Mariani G, Cotroneo P, Ghirlanda G, Clementi A, Andreani D, and Di Mario U.** Charge selectivity of proteinuria in type I diabetes explored by Ig subclass clearance. *Diabetes* 40: 1685-1690, 1991.
129. **Pisoni R, Ruggenenti P, Sangalli F, Lepre MS, Remuzzi A, and Remuzzi G.** Effect of high dose ramipril with or without indomethacin on glomerular selectivity. *Kidney Int* 62: 1010-1019, 2002.
130. **Pries AR, Secomb TW, and Gaehtgens P.** The endothelial surface layer. 440: 653, 2000.
131. **Pries AR, Secomb TW, Jacobs H, Sperandio M, Osterloh K, and Gaehtgens P.** Microvascular blood flow resistance: role of endothelial surface layer. 273: H2272, 1997.
132. **Remuzzi A, Fassi A, Bertani T, Perico N, and Remuzzi G.** ACE inhibition induces regression of proteinuria and halts progression of renal damage in a genetic model of progressive nephropathy. *Am J Kidney Dis* 34: 626-632, 1999.
133. **Rennke HG, Cotran RS, and Venkatachalam MA.** Role of molecular charge in glomerular permeability. Tracer studies with cationized ferritins. 67: 638, 1975.

134. **Rennke HG and Venkatachalam MA.** Glomerular permeability: in vivo tracer studies with polyanionic and polycationic ferritins. 11: 44, 1977.
135. **Rippe B and Haraldsson B.** Transport of macromolecules across microvascular walls: The two-pore theory. *Physiol Rev* 74: 163, 1994.
136. **Rippe B, Kamiya A, and Folkow B.** Transcapillary passage of albumin, effects of tissue cooling and of increases in filtration and plasma colloid osmotic pressure. 105: 171, 1979.
137. **Roselli S, Gribouval O, Boute N, Sich M, Benessy F, Attie T, Gubler MC, and Antignac C.** Podocin localizes in the kidney to the slit diaphragm area. *Am J Pathol* 160: 131-139, 2002.
138. **Rossing P, Rossing K, Jacobsen P, and Parving HH.** Unchanged incidence of diabetic nephropathy in IDDM patients. *Diabetes* 44: 739-743, 1995.
139. **Rostgaard J and Qvortrup K.** Electron microscopic demonstrations of filamentous molecular sieve plugs in capillary fenestrae. 53: 1, 1997.
140. **Rostgaard J and Qvortrup K.** Sieve plugs in fenestrae of glomerular capillaries-site of the filtration barrier? 170: 132, 2002.
141. **Ruggenti P, Mosconi L, Vendramin G, Moriggi M, Remuzzi A, Sangalli F, and Remuzzi G.** ACE inhibition improves glomerular size selectivity in patients with idiopathic membranous nephropathy and persistent nephrotic syndrome. *Am J Kidney Dis* 35: 381-391, 2000.
142. **Ruotsalainen V, Ljungberg P, Wartiovaara J, Lenkkeri U, Kestilä M, Jalanko H, Holmberg C, and Tryggvason K.** Nephrin is specifically located at the slit diaphragm of glomerular podocytes. 96: 7962, 1999.
143. **Russo LM, Bakris GL, and Comper WD.** Renal handling of albumin: a critical review of basic concepts and perspective. *Am J Kidney Dis* 39: 899-919, 2002.
144. **Scandling JD and Myers BD.** Glomerular size-selectivity and microalbuminuria in early diabetic glomerular disease. *Kidney Int* 41: 840-846, 1992.
145. **Schnitzer JE, Carley WW, and Palade GE.** Albumin interacts specifically with a 60-kDa microvascular endothelial glycoprotein. *Proc Natl Acad Sci U S A* 85: 6773-6777, 1988.
146. **Schnitzer JE, Carley WW, and Palade GE.** Specific albumin binding to microvascular endothelium in culture. *Am J Physiol* 254: H425-437, 1988.
147. **Schnitzer JE and Pinney E.** Quantitation of specific binding of orosomucoid to cultured microvascular endothelium: role in capillary permeability. *Am J Physiol* 263: H48-55, 1992.
148. **Schonherr E, Jarvelainen HT, Sandell LJ, and Wight TN.** Effects of platelet-derived growth factor and transforming growth factor-beta 1 on the synthesis of a large versican-like chondroitin sulfate proteoglycan by arterial smooth muscle cells. *J Biol Chem* 266: 17640-17647, 1991.

149. **Schonherr E, Kinsella MG, and Wight TN.** Genistein selectively inhibits platelet-derived growth factor-stimulated versican biosynthesis in monkey arterial smooth muscle cells. *Arch Biochem Biophys* 339: 353-361, 1997.
150. **Segev Y, Landau D, Rasch R, Flyvbjerg A, and Phillip M.** Growth hormone receptor antagonism prevents early renal changes in nonobese diabetic mice. 10: 2374, 1999.
151. **Selby JV, FitzSimmons SC, Newman JM, Katz PP, Sepe S, and Showstack J.** The natural history and epidemiology of diabetic nephropathy. Implications for prevention and control. *Jama* 263: 1954-1960, 1990.
152. **Sharma K, McCue P, and Dunn SR.** Diabetic kidney disease in the db/db mouse. *Am J Physiol Renal Physiol* 284: F1138-1144, 2003.
153. **Sharma K and Ziyadeh FN.** Hyperglycemia and diabetic kidney disease. The case for transforming growth factor-beta as a key mediator. *Diabetes* 44: 1139-1146, 1995.
154. **Sharma K and Ziyadeh FN.** Renal hypertrophy is associated with upregulation of TGF-beta 1 gene expression in diabetic BB rat and NOD mouse. *Am J Physiol* 267: F1094-1001, 1994.
155. **Sharma K, Ziyadeh FN, Alzahabi B, McGowan TA, Kapoor S, Kurnik BR, Kurnik PB, and Weisberg LS.** Increased renal production of transforming growth factor-beta1 in patients with type II diabetes. *Diabetes* 46: 854-859, 1997.
156. **Shih NY.** CD2AP localizes to the slit diaphragm and binds to nephrin via a novel C-terminal domain. 159: 2303, 2001.
157. **Shih NY, Li J, Karpitskii V, Nguyen A, Dustin ML, Kanagawa O, Miner JH, and Shaw AS.** Congenital nephrotic syndrome in mice lacking CD2-associated protein. *Science* 286: 312-315, 1999.
158. **Soulis T, Cooper ME, Vranes D, Bucala R, and Jerums G.** Effects of aminoguanidine in preventing experimental diabetic nephropathy are related to the duration of treatment. *Kidney Int* 50: 627-634, 1996.
159. **Spencer MW, Muhlfeld AS, Segerer S, Hudkins KL, Kirk E, LeBoeuf RC, and Alpers CE.** Hyperglycemia and hyperlipidemia act synergistically to induce renal disease in LDL receptor-deficient BALB mice. *Am J Nephrol* 24: 20-31, 2004.
160. **Steffes MW, Schmidt D, McCrery R, and Basgen JM.** Glomerular cell number in normal subjects and in type 1 diabetic patients. *Kidney Int* 59: 2104-2113, 2001.
161. **Stolte H, Schurek HJ, and Alt JM.** Glomerular albumin filtration: a comparison of micropuncture studies in the isolated perfused rat kidney with in vivo experimental conditions. 16: 377, 1979.
162. **Strippoli GF, Di Paolo S, Cincione R, Di Palma AM, Teutonico A, Grandaliano G, Schena FP, and Gesualdo L.** Clinical and therapeutic aspects of diabetic nephropathy. *J Nephrol* 16: 487-499, 2003.

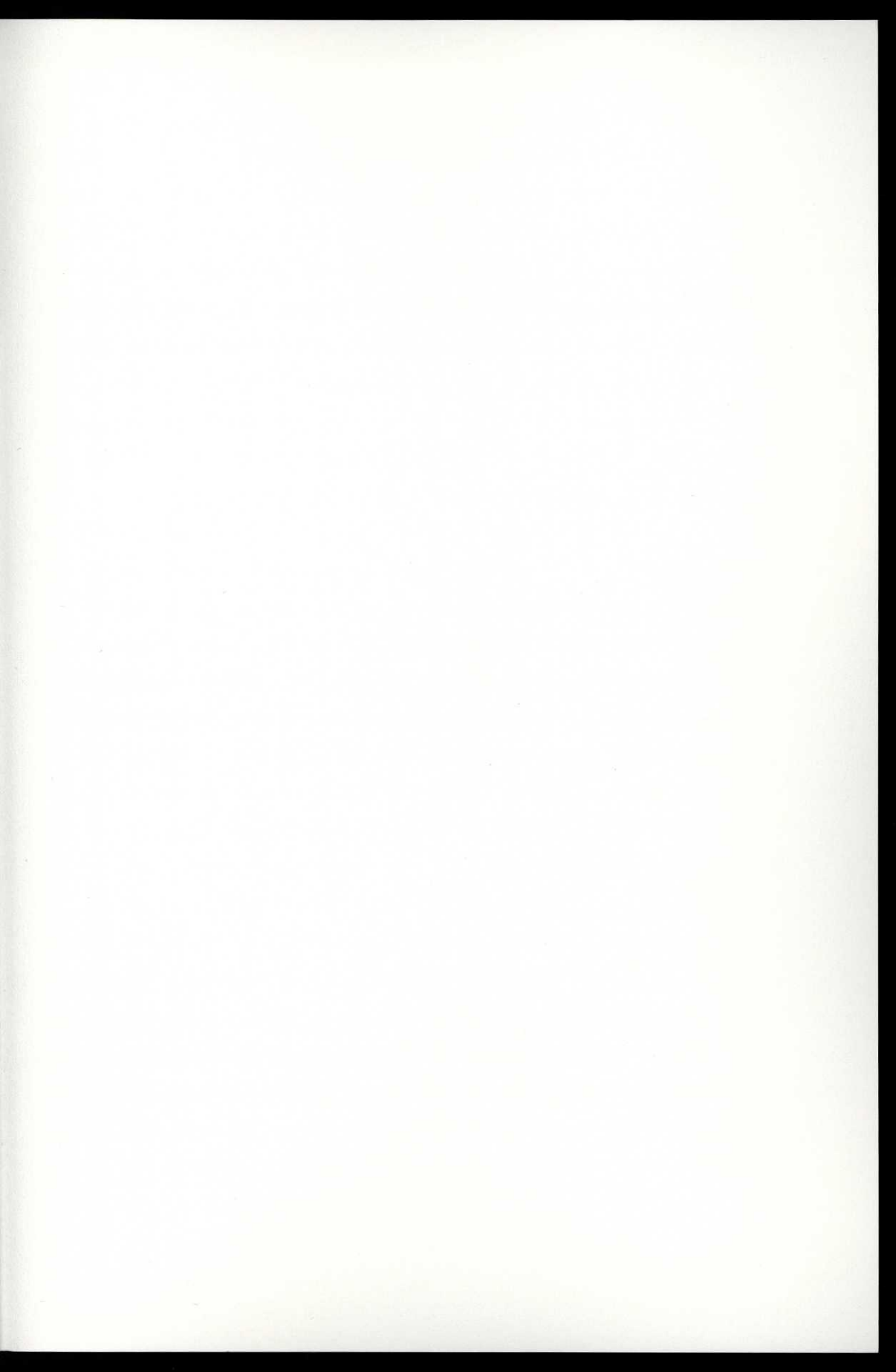
163. **Sörensson J, Ohlson M, and Haraldsson B.** A quantitative analysis of the glomerular charge barrier in the rat. 280: F646, 2001.
164. **Sörensson J, Ohlson M, Lindström K, and Haraldsson B.** Glomerular charge selectivity for horseradish peroxidase and albumin at low and normal ionic strengths. 163: 83, 1998.
165. **Tojo A and Endou H.** Intrarenal handling of proteins in rats using fractional micropuncture technique. 263: F601, 1992.
166. **Tomlanovich S, Deen WM, Jones HW, 3rd, Schwartz HC, and Myers BD.** Functional nature of glomerular injury in progressive diabetic glomerulopathy. *Diabetes* 36: 556-565, 1987.
167. **Torffvit O and Rippe B.** Size and charge selectivity of the glomerular filter in patients with insulin-dependent diabetes mellitus: urinary immunoglobulins and glycosaminoglycans. 83: 301, 1999.
168. **Tryggvason K and Wartiovaara J.** Molecular basis of glomerular permselectivity. *Curr Opin Nephrol Hypertens* 10: 543-549, 2001.
169. **Tsuchida K, Makita Z, Yamagishi S, Atsumi T, Miyoshi H, Obara S, Ishida M, Ishikawa S, Yasumura K, and Koike T.** Suppression of transforming growth factor beta and vascular endothelial growth factor in diabetic nephropathy in rats by a novel advanced glycation end product inhibitor, OPB-9195. *Diabetologia* 42: 579-588, 1999.
170. **Turley EA.** Hyaluronan and cell locomotion. *Cancer Metastasis Rev* 11: 21-30, 1992.
171. **Wahab NA, Harper K, and Mason RM.** Expression of extracellular matrix molecules in human mesangial cells in response to prolonged hyperglycaemia. *Biochem J* 316 (Pt 3): 985-992, 1996.
172. **Valiyaveetil M, Achur RN, Muthusamy A, and Gowda DC.** Chondroitin sulfate proteoglycans of the endothelia of human umbilical vein and arteries and assessment for the adherence of Plasmodium falciparum-infected erythrocytes. *Mol Biochem Parasitol* 134: 115-126, 2004.
173. **Wang J, Takeuchi T, Tanaka S, Kubo SK, Kayo T, Lu D, Takata K, Koizumi A, and Izumi T.** A mutation in the insulin 2 gene induces diabetes with severe pancreatic beta-cell dysfunction in the Mody mouse. *J Clin Invest* 103: 27-37, 1999.
174. **Weigert C, Brodbeck K, Klopfer K, Haring HU, and Schleicher ED.** Angiotensin II induces human TGF-beta 1 promoter activation: similarity to hyperglycaemia. *Diabetologia* 45: 890-898, 2002.
175. **Wight TN.** Versican: a versatile extracellular matrix proteoglycan in cell biology. *Curr Opin Cell Biol* 14: 617-623, 2002.
176. **Wight TN and Merrilees MJ.** Proteoglycans in atherosclerosis and restenosis: key roles for versican. *Circ Res* 94: 1158-1167, 2004.

177. **Vijan S and Hayward RA.** Treatment of hypertension in type 2 diabetes mellitus: blood pressure goals, choice of agents, and setting priorities in diabetes care. *Ann Intern Med* 138: 593-602, 2003.
178. **Wilson KH, Eckenrode SE, Li QZ, Ruan QG, Yang P, Shi JD, Davoodi-Semiromi A, McIndoe RA, Croker BP, and She JX.** Microarray analysis of gene expression in the kidneys of new- and post-onset diabetic NOD mice. *Diabetes* 52: 2151-2159, 2003.
179. **Vink H and Duling BR.** Capillary endothelial surface layer selectively reduces plasma solute distribution volume. 278: H285, 2000.
180. **Vink H and Duling BR.** Identification of distinct luminal domains for macromolecules, erythrocytes, and leukocytes within mammalian capillaries. 79: 581, 1996.
181. **Wolf J, Lilly F, and Shin SI.** The influence of genetic background on the susceptibility of inbred mice to streptozotocin-induced diabetes. *Diabetes* 33: 567-571, 1984.
182. **Vorbrodt AW.** Ultracytochemical characterization of anionic sites in the wall of brain capillaries. 18: 359, 1989.
183. **Yamaguchi Y, Mann DM, and Ruoslahti E.** Negative regulation of transforming growth factor-beta by the proteoglycan decorin. *Nature* 346: 281-284, 1990.
184. **Yamamoto T, Noble NA, Cohen AH, Nast CC, Hishida A, Gold LI, and Border WA.** Expression of transforming growth factor-beta isoforms in human glomerular diseases. *Kidney Int* 49: 461-469, 1996.
185. **Yoshioka M, Kayo T, Ikeda T, and Koizumi A.** A novel locus, Mody4, distal to D7Mit189 on chromosome 7 determines early-onset NIDDM in nonobese C57BL/6 (Akita) mutant mice. *Diabetes* 46: 887-894, 1997.
186. **Zheng F, Cai W, Mitsuhashi T, and Vlassara H.** Lysozyme enhances renal excretion of advanced glycation endproducts in vivo and suppresses adverse age-mediated cellular effects in vitro: a potential AGE sequestration therapy for diabetic nephropathy? *Mol Med* 7: 737-747, 2001.
187. **Zheng F, He C, Cai W, Hattori M, Steffes M, and Vlassara H.** Prevention of diabetic nephropathy in mice by a diet low in glycooxidation products. 18: 224, 2002.

På grund av upphovsrättsliga skäl kan vissa ingående delarbeten ej publiceras här.
För en fullständig lista av ingående delarbeten, se avhandlingens början.

Due to copyright law limitations, certain papers may not be published here.
For a complete list of papers, see the beginning of the dissertation.





ISBN 91-628-6485-8